2014-10-29

The Influence of Social Environment and Hypercholesterolemia on Sympathetic Nervous System Innervation of Vascular Tissue in Rabbits

Crystal Noller
University of Miami, crystal.noller@gmail.com

UNIVERSITY OF MIAMI

THE INFLUENCE OF SOCIAL ENVIRONMENT AND HYPERCHOLESTEROLEMIA ON SYMPATHETIC NERVOUS SYSTEM INNERVATION OF VASCULAR TISSUE IN RABBITS

By

Crystal M. Noller

A DISSERTATION

Submitted to the Faculty
of the University of Miami
in partial fulfillment of the requirements for
the degree of Doctor of Philosophy

Coral Gables, Florida

December 2014

UNIVERSITY OF MIAMI

A dissertation submitted in partial fulfillment of
the requirements for the degree of
Doctor of Philosophy

THE INFLUENCE OF SOCIAL ENVIRONMENT AND HYPERCHOLESTEROLEMIA ON SYMPATHETIC NERVOUS SYSTEM INNERVATION OF VASCULAR TISSUE IN RABBITS

Crystal M. Noller

Approved:

_____
Philip M. McCabe, Ph.D.
Professor of Psychology

_____
Armando J. Mendez, Ph.D.
Research Associate Professor of Medicine

_____
Neil Schneiderman, Ph.D.
Professor of Psychology

_____
Julia Zaias, D.V.M., Ph.D.
Research Associate Professor of Pathology

_____
Maria M. Llabre, Ph.D.
Professor of Psychology

_____
M. Brian Blake, Ph.D.
Dean of the Graduate School

_____
Michael H. Antoni, Ph.D.
Professor of Psychology

NOLLER, CRYSTAL M. (Ph.D., Psychology)
The Influence of Social Environment and Hypercholesterolemia on Sympathetic Nervous System Innervation of Vascular Tissue in Rabbits. (December 2014)

Abstract of a dissertation at the University of Miami.

Dissertation supervised by Professor Philip M. McCabe.
No. of pages in text. (68)

Behavioral and psychosocial factors have been shown to influence cardiovascular disease. While interventions targeting these risk factors demonstrate clinical improvement, mechanisms underlying these effects remain to be determined. Research has also defined a relationship between psychosocial stress and immune function, and revealed stress related increases in lymphatic sympathetic nerve density. Considering that inflammation characterizes the various stages of heart disease, the current study assessed whether social stress could influence vascular sympathetic innervation in the presence or absence of hypercholesterolemia. We found dense sympathetic innervation extending into the vascular media and intima throughout the aortic arch and thorax in diseased as well as non-diseased animals. To our knowledge, this is the first demonstration of extensive sympathetic innervation in all layers of normal vessels. Compared to NZW animals, WHHL rabbits displayed increased sympathetic innervation and a relationship between sympathetic varicosity counts and lesion severity, suggesting that innervation increases with hypercholesterolemia and advanced disease. In hypercholesterolemic animals, rabbits within a socially unstable environment showed more agonistic behavior and atherosclerosis than rabbits in a socially stable condition. Contrary to our hypothesis, however, we did not find evidence for an effect of social environment on sympathetic innervation. Reasons for this null outcome are proposed and alternative mechanistic links

between social behavior and heart disease are discussed. This novel study provided insight on the brain-immune connection within the vasculature, identifying factors influencing innervation density, and potentially mediating disease.

TABLE OF CONTENTS

LIST OF TABLES

LIST OF FIGURES

Page

Chapter 1: Introduction

Heart disease is and has been the leading cause of death in the United States (Heron, 2012; Heron, 2013; Hoyert & Xu, 2012; Murphy, Xu, & Kochanek, 2013). Recent data has shown a decrease in CVD death rates over the past ten years, however, even with that decline, cardiovascular disease accounted for about 1 in every 3 deaths in 2010 (Go et al., 2014). Negative health behaviors such as poor diet, lack of physical activity, and tobacco use can increase the risk for heart disease and other chronic illnesses (Hemingway & Marmot, 1999; Kaplan, 2009; Mokdad, Marks, Stroup, & Gerberding, 2004). Research has also shown that psychosocial factors, including depressed affect, hopelessness, hostility, denial, and poor social support, are associated with incidence and increased severity of several chronic diseases, including coronary heart disease (CHD), cancer, and HIV-AIDS (House, Landis, & Umberson, 1988; Gidron & Ronson, 2008; Leserman et al., 2000; Schneiderman, 2004).

Clinical trials designed to reduce stress and hostility after myocardial infarction (MI) have demonstrated effectiveness by decreasing the number of recurrent MI and cardiovascular disease (CVD) events in patients receiving cognitive behavioral therapy in additional to standard care (Gulliksson et al., 2011), further supporting the idea that targeting traditional risk factors alone may not be sufficient to improve clinical outcome after MI. Clinical research has suggested protective associations between integrated social networks and a decrease in cardiac as well as all-cause mortality, and has depicted a prognostic relationship between the lack of functional social support and the occurrence of CHD (Barth, Schneider, & Von Känel, 2010).

Social Environment and the Progression of Heart Disease

In order to understand the mechanistic role of social/emotional factors in the progression of disease, animal work is often necessary. In a seminal paper, Kaplan and colleagues (1982) examined the influence of social stress in monkeys, using a model of dietary induced atherosclerosis. Dominant male monkeys within an unstable social environment developed twice the coronary atherosclerosis compared to monkeys housed in a socially stable environment, a finding that was independent of serum lipid concentrations or blood pressure. Dominant monkeys in the unstable group also displayed more contact aggression than those in the stable group and more severe atherosclerosis when compared to subordinate animals within the unstable group (Kaplan, Manuck, Clarkson, Lusso, & Taub, 1982; Kaplan & Manuck, 1999).

In a later study, the influence of social stress on atherosclerosis was examined in normocholesterolemic monkeys. Again, it was found that animals in the stressed condition had more coronary artery atherosclerosis, demonstrated by increased intimal area and intimal thickness, as well as more advanced lesions compared to those in the unstressed condition. There was no significant group difference in total serum cholesterol, HDLC, fasting glucose, ratio of body weight to body length, or systolic and diastolic blood pressure (Kaplan et al., 1983), suggesting that social stress alone was enough to exacerbate disease without the influence of traditional risk factors.

Other work has examined how behavioral factors contribute to the progression of atherosclerosis in a genetic model, the Watanabe Heritable Hyperlipidemic (WHHL) rabbit, using male rabbits housed in stressful, supportive, or isolated social environments (McCabe et al., 2002). This study once again demonstrated that animals housed in a

stable environment had significantly less aortic atherosclerosis compared to the other two groups. While unstable and isolated groups had comparable lesion areas, animals within the unstable group displayed more severe lesions.

Behavior in each of these groups reflected the social environment paradigm; the unstable group spent more time in agonistic behavior, the stable group more time in affiliative behavior, and the isolated group in inactivity. Physiological measures reflected chronic hypothalamic-pituitary-adrenal (HPA) axis activity, where animals in the unstable group showed an increase in corticosterone compared to the individually caged animals, as well as heavier adrenal glands and increased testicular weight compared to the other two groups. Interestingly, the unstable group had a lower mean arterial blood pressure at the end of the study, while the individually caged animals had increased heart rate compared to the unstable group, suggesting that hemodynamic variables were not responsible for increased severity of disease, at least within the unstable group (McCabe et al., 2002).

Stress as a Contributing Factor to the Progression of Heart Disease

The previous studies indicate that social stress, in the presence, as well as absence of high cholesterol can exacerbate the progression of atherosclerosis. This outcome appears to be independent of changes in blood pressure, as well as other traditional risk factors. Thus far, the mechanism responsible for these findings remains elusive. Exacerbation of the HPA axis during times of chronic stress may be one mechanism. In fact, research has shown that the presence of a bonding partner can reduce the neuroendocrine response to a stressful situation in animals (Sachser, Dürschlag, & Hirzel, 1998); and that pro-social behavior suppresses HPA axis activity in animals as well as in

humans (reviewed in DeVries, Glasper, & Detillion, 2003). Thus, social support may serve a cardio-protective role indirectly by diminishing the physiological stress response.

The preceding studies demonstrate a change in peripheral indicators of HPA activity (e.g., glucocorticoids) as a result of social factors. We have previously described such differences as a function of differing social environments. Rabbits housed in an unstable social environment displayed physiological responses characteristic of chronic stress; increased urinary norepinephrine, plasma cortisol, and splenic weight, and a decrease in body weight and visceral fat compared to rabbits housed in a stable social environment or social isolation (Noller et al., 2013).

The preceding studies clearly confirm the well-known physiological response to stress. It is possible, however, that the mechanism responsible for the increase in severity of atherosclerosis found in unstable social environments may be due to specific changes occurring within the vessel wall. Clinical research has shown that stress can induce endothelial dysfunction, both by way of physiologically induced SNS activity (i.e., lower body negative pressure box) as well as by increased psychological distress (Hijmering et al., 2002; Spieker et al., 2002, respectively).

Adrenergic influence within the vasculature has also been shown in other animal studies. Skantze and colleagues (1998) reported that psychosocial stress led to an increase in the number of damaged thoracic endothelial cells in the aorta. This finding in monkeys was independent of excessive dietary cholesterol intake, demonstrating an influence of stress in the absence of hypercholesterolemia. Treatment with β1-blocker significantly inhibited this effect, an outcome demonstrating the anti-atherosclerotic effects previously ascribed to these drugs (Bondjers, 1994). Furthermore, by demonstrating a decrease in

the number of damaged cells, the outcome of this study mechanistically supports the widespread clinical use of β-blockers for persons at risk for CVD (Frishman, 2003). However, as no group differences in blood pressure were reported, the decrease in damaged endothelial cells may have been through a concurrent decrease in blood pressure, as has been previously reported for β1-blockers (Taverner, Mackay, Craig, & Watson, 1991).

Previous reports have shown that stress is related to severity of disease and endothelial function. Williams and colleagues (1991) reported that when combined with a high-cholesterol diet, stress was related to increased plaque size. Independent of diet, they also showed a stress-related decreased vascular responsivity to the vasodilator, acetylcholine. Other researchers showed the importance of stress duration, where a normal vasodilatory response was reported in animals experiencing early but not late stress, suggesting that an altered endothelial response is potentially reversible (Williams, Kaplan, & Manuck, 1993). Importantly, this outcome was found to be dependent on present stress, as no significant differences were found between the early- and late- stress groups in cardiovascular measures (i.e., blood pressure and resting heart rate), or other risk factors such as total or HDL cholesterol levels. Taken together, research supports the idea that stress, in the presence as well as absence of traditional risk factors, can induce potentially pro-atherogenic physiological changes within the vessel wall.

Inflammation as a Contributing Factor to the Progression of Heart Disease

The pathophysiology of coronary artery disease is initially comprised of damage to the endothelium, in turn triggering a cascade of pro-atherogenic events, including increasing the expression of adhesion molecules within the vessel wall (Libby &

Theroux, 2005). The idea that atherosclerosis is marked by a heightened inflammatory state has been reviewed extensively (Libby, Ridker, & Maseri, 2002; Libby, Ridker, & Hansson, 2009; Libby, Ridker, & Hansson, 2011; Ross, 1999) and supports the idea that inflammation is present both systemically, as well as locally within the vessel. In fact, inflammatory cell participation has been found throughout the various stages of the disease, from initial endothelial dysfunction to fibrous cap formation (reviewed by Libby et al., 2002). In addition, increased C-reactive protein levels, indicative of low-grade circulating inflammation, increases the risk of CHD two- to three-fold in clinical populations (Danesh et al., 2000; Koenig, Meisinger, Baumert, Khuseyinova, & Löwel, 2005).

Previous studies have described a link between long-term social stress and immunity. Cohen and colleagues (1992) reported that nonhuman primates in an unstable social environment demonstrated a decreased immune response compared to animals housed in a stable social environment. The question at hand is specifically how social stress affects the immune response. One such possibility is through remodeling of the sympathetic nervous system.

It has been shown that behavioral stress can affect the density of lymphatic catecholaminergic nerve fibers (reviewed by Sloan, Capitanio, & Cole, 2008). Sloan et al. (2007) reported an increase in the density of lymph node catecholaminergic nerve fibers in animals housed in unstable social environments, where there was a remarkable 80% increase in catecholaminergic varicosities. It was also found that social stress increased viral replication of simian immunodeficiency virus (SIV) by 58%, while no significant

difference was found between groups in the overall frequency of immune cells examined; macrophages, T- or B-lymphocytes, or follicular dendritic cells within lymph node tissue.

Sympathetic neurons contain varicosities along the axon where nerve terminals are formed and synapse on adjacent cells and pre-synaptic nerves. These terminals contain synaptic vesicles storing neurotransmitters released upon excitation of the nerve. Sympathetic/catecholaminergic nerves derive their name from their ability to release catecholamines, namely norepinephrine.

In a later study, sympathetic innervation of lymphoid tissue varied as a function of social temperament, defined as a propensity to socially affiliate (termed "Sociability"). A 2.8-fold increase was found in the density of catecholaminergic innervation in tissues from Low Sociable animals compared to High Sociable animals, along with a 2.3-fold increase in the expression of nerve growth factor (NGF) mRNA, a neurotrophic factor critical for the support of peripheral sympathetic nerve fibers (Levi-Montalcini, 1987; Fariñas, 1999). Low Sociable animals showed a decreased response to tetanus vaccination, as well as increased expression of the immunoregulatory cytokine genes IL-4 and IFN-γ (Sloan, Capitanio, Tarara, & Cole, 2008). Results from the previous studies describe alterations in sympathetic innervation that may prove especially relevant in understanding how stress and behavioral factors influence the course of disease.

Alterations in Sympathetic Innervation in Various Disease States

In addition to previous reports on SIV, enhanced sympathetic innervation has been linked to advancement of other chronic diseases, such as cancer. Several reviews have described the influence of the sympathetic nervous system on cancer progression in experimental as well as clinical studies (Tilan & Kitlinska, 2010; Pimentel, Chai, Le,

Cole, & Sloan, 2012). Sloan and colleagues (2010) showed a direct effect of the sympathetic nervous system on breast cancer metastasis. In their animal model, female mice experiencing chronic stress demonstrated a 38-fold increase in metastasis of primary breast tumor cells compared to controls. Importantly, there was an increase in recruitment of macrophages relative to controls; where specifically, a 53% increase in mammary tumor infiltration of macrophages was shown.

This finding is important as it suggests an interaction between macrophages and stress-related advancement of disease. It also supports a modulatory role of the sympathetic nervous system on immune cells, identifying macrophages as specific targets. It has been shown that sympathetic nerves regulate the local recruitment of leukocytes through β-adrenergic signaling (Scheiermann et al., 2012). Straub et al. (2000) demonstrated that sympathetic neurotransmitters could elicit monocyte and macrophage chemotaxis. Thus, increased sympathetic innervation could lead to recruitment and activation of monocytes/macrophages, thereby advancing the progression of atherosclerosis.

Previously described research has suggested a relationship between macrophages and increased sympathetic innervation. Indeed, in a model of myocardial infarction, it has been shown that depletion of macrophages resulted in a lack of sympathetic hyperinnervation at the site of ischemic injury, corresponding with a reduction in NGF levels (Wernli, Hasan, Bhattacherjee, van Rooijen, & Smith, 2009). Taken together, these studies demonstrate a critical role of macrophages in propelling sympathetic innervation, and suggest that chronic stress may advance atherosclerosis by affecting macrophages present within the lesion.

Sympathetic Innervation in Coronary Blood Vessels

Previous research has indicated that sympathetic innervation of coronary blood vessels is predominantly confined to the adventitial-medial border (Santer, 1982; Scott, Honey, Martin, & Booth, 1992). Recent work has also shown sympathetic innervation extending into the media (Ogeng'o, Malek, & Kiama, 2011). The location of sympathetic nerve density in the blood vessel supports its vasoconstriction role (reviewed in Kreulen, 2003).

Previous work has shown a relationship between innervation and vascular damage. Scott et al. (1992) demonstrated that damage to the vessel wall of carotid arteries resulted in intimal thickening and perivascular nerve degeneration. Additionally, it has been shown in the heart that sympathetic innervation increased as a response to hypercholesterolemia (Liu et al., 2003; Luo, Wu, Liu, Fu, & Su, 2004). However, it is unknown how social stress affects vascular sympathetic innervation, and whether this influence is contingent on other factors, such as hypercholesterolemia.

Rationale

The critical discovery that social stress can induce an increase in sympathetic innervation identifies an important, and perhaps overlooked, behavioral component of immunity. It also isolates an imperative question in cardiovascular research relating social environment, stress, and CVD occurrence. If an increase in lymphatic sympathetic innervation as well as viral replication was found in animals housed in socially stressful conditions (Sloan et al., 2007), is it possible that an increase in vascular sympathetic innervation could characterize an unstable social environment, and potentially be the

mechanism responsible for an increase in the severity of atherosclerosis previously described in unstable social environments (Kaplan et al., 1982; McCabe et al., 2002)?

There is evidence to suggest that a relationship between immune cells and nerve fibers may be dependent on the presence of diseased tissue. In a study examining normal (lesion types 0 and I) and atherosclerotic (lesion types II, III, and IV) coronary segments, researchers found an increase in mast cells and connecting sensory nerve fibers in grade IV compared to grades II and III lesions, as well as compared to normal vessels (Laine, Naukkarinen, Heikkilä, Penttilä, & Kovanen, 2000). It remains unknown whether this relationship exists with sympathetic nerve fibers and how either branch of the autonomic nervous system differentially innervates coronary blood vessels.

Previous data demonstrate an increase in sensory innervation in the presence of disease (Laine et al., 2000) and identifies a role for immune cells to affect innervation by way of NGF release (Sloan et al., 2008). Should this relationship exist with sympathetic nerves, we would expect to see a concurrent increase in innervation along with disease, that is, in areas with infiltrating macrophages. In fact, Sloan et al. (2007) reported the presence of immune cells in regions of increased innervation, specifically T-lymphocytes and macrophages.

It is likely then, that these macrophages, present in atherosclerosis (Libby, 2012), would further propel innervation by the release of NGF (Wernli et al., 2009), and that stress may exacerbate this release (Caroleo, Costa, Bracci-Laudiero, & Aloe, 2001). Indeed, it has been shown that LPS, a potent inflammatory inducing agent, can stimulate human macrophages to produce NGF (Caroleo et al., 2001). Perhaps more importantly, research has shown that after MI, depletion of macrophages in the heart not only reduces

levels of NGF, but also leads to decreased sympathetic axon densities in rats (Wernli et al., 2009). Thus, the same mechanisms present in previously reported studies exist within the vasculature; in turn supporting the idea that enhanced sympathetic innervation promotes atherosclerotic advancement.

Although there are similarities between atherosclerosis and other disease states demonstrating sympathetic remodeling, it is unknown whether the similarities are sufficient to produce a comparable response. Thus, several important questions remain to be answered. Namely, whether social environment influences patterns of vascular innervation in the same way previously reported in the lymph nodes (Sloan et al., 2007), whether this relationship is dependent on other factors (e.g., presence of activated macrophages), or whether hyperinnervation can be induced by stress alone.

Thus, the aim of the current study was to examine vascular sympathetic innervation patterns in two strains of rabbit, Watanabe Heritable Hyperlipidemic (WHHL) and New Zealand White (NZW) rabbits, both housed in differing social environments (e.g., unstable and stable social conditions). We assessed whether an increase in innervation density was driven by differences in social stress, atherosclerotic disease, or a combination of these two factors. Additionally, we examined differences in innervation patterns within two areas of the aorta, the aortic arch and the thoracic area, as previous work has shown that early disease processes begin in the arch (reviewed in Aliev et al., 2004), and that the arch is the aortic area that develops the most extensive lesions (Buja, Kita, Goldstein, Watanabe, & Brown, 1983).

This novel study provided necessary insight on the mechanistic links between social behavior and atherosclerosis. Considering that heart disease is still a leading cause

of death in the U.S., insight on the brain-immune connection within the vasculature is relevant and much needed.

The Current Study:

The purpose of the current study was to characterize vascular sympathetic innervation in normal versus hypercholesterolemic blood vessels, and examine innervation as a function of social stress and the presence or absence of disease.

The aims of the study were as follows:

1. To examine regional differences in sympathetic innervation in different regions of the aorta (e.g., arch versus thorax)
2. To examine the influence of disease on sympathetic innervation
3. To examine the relationship between disease severity and sympathetic innervation
4. To examine the influence of social environment on sympathetic innervation
5. To examine the interaction between social environment and disease
6. To examine the relationship between innervation patterns and parameters characterizing disease (e.g., cholesterol and triglycerides) and unstable social environments (e.g., cortisol).

We had three main hypotheses:

H1: Vascular innervation density is more pronounced in major aortic regions that develop the most severe lesions. We expected this outcome in WHHL but not NZW rabbits, due to strain differences in lesion severity.

H2: Vascular innervation is driven by the presence of disease (hypercholesterolemia versus normal rabbit strain).

H3: Vascular innervation is exacerbated by an interaction between disease and social stress. We predicted that in the presence of disease, an unstable social environment would advance sympathetic innervation more rapidly than a stable social environment. We did not expect to find an influence of social environment within the NZW group, due to the lack of NGF producing macrophages in this group lacking disease.

Chapter 2: Method

Animals

All procedures were approved by the Animal Care and Use Committee of the University of Miami. A total of 46 animals were included in the current study, 22 of the Watanabe heritable hyperlipidemic (WHHL) strain and 24 of the New Zealand White (NZW) strain, all purchased through Covance Research Products, Inc (Denver, PA). After acclimation, male rabbits (2.5-3 months old, approximately 1.5-2 kg) were semi-randomly assigned to either unstable or stable social conditions, based on birth records of available animals. That is, the stable group consisted of littermate pairs while the unstable group contained non-littermates. The size of resultant social groups were as follows: within the WHHL group, 12 animals were assigned to an unstable environment and 10 animals to a stable environment, and within the NZW group, 14 animals to an unstable environment and 10 animals to a stable environment.

We have previously reported comparable stress responses between these two strains of rabbit (Szeto et al., 2004), and thus, did not anticipate differing effects of social environments between strains. The experimental and social-behavioral paradigms have been previously described in detail (McCabe et al., 2002; Noller et al., 2013). Briefly, over the course of the study (approximately 16-20 weeks), rabbits were paired for four hours every day, as follows.

Social Environment Paradigm

Rabbits in the unstable group were paired with an unfamiliar non-littermate rabbit; pairings of which were switched weekly, forcing the rabbits to continually re-

establish dominant/subordinate relationships. Rabbits in the stable group were paired with the same littermate rabbit each day. Rabbits in the wild live in warrens with potentially hundreds of family members. Although they are social creatures, rabbits are territorial and aggressive while establishing dominance-subordinance hierarchies within the group (especially males) (Lockley, 1961; Myktowycz & Hesterman, 1975). Thus, pairings in both groups alternated between home and away cages, ensuring that no rabbit obtained a systematic home/intruder advantage.

Behavior was scored three times per week for each animal during the first 10 minutes of pairing and classified into the following major categories: agonistic behavior, affiliative behavior, other nonagonistic behavior, and inactivity. Agonistic behaviors included biting, combat, chasing, escaping, escape mounting, mounting, enuresis, approaching, aggressive grooming, freezing, attempting to mount, and thumping. Affiliative behaviors included mutual passive rest, nuzzling, and sniffing or grooming. Other non-agonistic behavior included circling, self-grooming, leaping, and cage exploration. Inactivity consisted of passive rest and sitting quietly in the cage.

Gross Examination of Atherosclerotic Lesion

Gross examination of aortic areas were independently evaluated and measured by a pathologist (J.Z.) blind to social condition according to AHA guidelines (Stary et al., 1994; Stary et al., 1995). Total lesion area (mm^2) for the arch and thoracic sections were determined, representing a global disease score. By definition, we expected the NZW rabbits to have little or no disease; however, all animals in the study were evaluated. Examination confirmed very minimal disease in the NZW group (representing < 2 mm^2 throughout both regions combined for all animals in this group).

Sample Selection and Preparation

All immunohistochemistry, microscopy, regions of interest, histology, data processing, and quantification were performed blind to social environment assignment. Without knowledge to social environment, rabbits were assigned a four-digit number. Tissue blocks and slides were labeled according to this identifier. Data were decoded after quantification and prior to group analyses.

Three to four mm sections of aortic tissue were formalin fixed and embedded in paraffin blocks for cross-sectional slicing. Representative blocks from each tissue location (e.g., aortic arch and thoracic aorta) were selected for each rabbit. Tissues were mounted on glass slides, using a microtome to slice 10 μm sections. Twenty-six slides from each animal were prepared for each of the two tissue locations. Using the Systematic-Random Sampling method (Mouton, 2002), every 5^{th} slide was selected for immunohistochemical processing (e.g., slides 1, 6, 11, 16, and 21).

Thus, five slides per animal, per location, were immunohistochemically stained, and the best three slides (i.e., least bubbles in the mounting media, least folds in the tissue) were identified by light microscopy and used for quantification. The last slide per animal per aortic area (e.g., number 26) was processed for histology by hematoxylin and eosin (H&E) staining, and one slide per strain per staining day served as an isotype control to examine specificity of the antibody. Across the entire study, a total of 2392 slides were prepared (26 slides for 46 animals in both aortic areas), and 460 slides (5 slides for each of two sections, for 46 animals) were stained using the following standard lab procedure.

Portions of the image with damage (e.g., folds in the tissue, bubbles in the mounting media, etc.) were excluded. These regions were minimal and represented less than 1.5% of total available area. Vascular tissues were unavailable for two WHHL rabbits, representing one arch section and one thoracic section; thus, these animals were excluded from these regions.

Immunohistochemistry (IHC)

Prior to staining, samples were deparaffinized using an automated instrument (Leica JUNG Autostainer XL). We performed antigen retrieval by placing slides in citrate solution (0.01 M citric acid, 0.05% Tween 20, pH = 6) and heating under pressure for 20 minutes at 120'C. Slides were cooled for 30 minutes, rinsed with $_{dd}H_20$ then phosphate buffered saline (PBS), and finally washed with wash buffer (BioGenex, Fremont, CA). A universal blocking solution was used to reduce non-specific background staining (BioGenex power block, Fremont, CA).

Slides were again washed with wash buffer, incubated with blocking solution against proteins from the secondary antibody host (e.g., donkey serum), and incubated overnight at 4℃ with either primary antibodies or non-immune antibody isotype controls (1 μg/ml; Jackson ImmunoResearch Laboratories, Inc., West Grove, PA) for the primary antibody host (e.g., chicken and guinea pig), diluted in antibody diluent (1% BSA). To identify sympathetic varicosities, we used the following primary antibodies: chicken α-tyrosine hydroxylase (1:500; Millipore, Billerica, MA), an enzyme precursor for catecholamines, and guinea pig α-synapsin (1:250; Synaptic Systems, Germany), a protein axonal marker.

On the second day, slides were washed with wash buffer, incubated with secondary antibodies for 2 hours, and washed with wash buffer and PBS. Finally, slides were mounted with ProLong Gold with DAPI (4',6-diamidino-2-phenylindole) to stain cell nuclei (Invitrogen, Grand Island, NY), allowed to cure for 24 hours and sealed. Immunostaining was visualized by fluorescence microscopy using the following secondary antibodies: tyrosine hydroxylase was detected using donkey α-chicken AlexaFluor 594 nm (1:300; Jackson ImmunoResearch Laboratories, Inc., West Grove, PA) and synapsin was detected with donkey α-guinea pig AlexaFluor 647 nm (1:450; Jackson ImmunoResearch Laboratories, Inc., West Grove, PA).

Microscopy

Images were acquired for quantification of nerve terminals using an Olympus immunofluorescence microscope. Tiled images were acquired for each slide; the use of a 10x objective lens resulted in a 643.04 nm/ pixel size resolution. Every image contained three channels, representing a distinct fluorescent probe; channel 1 with tyrosine hydroxylase, channel 2 with synapsin, and channel 3 with cell nuclei staining.

High resolution images were acquired using a Leica SP5 inverted confocal microscope with 20x/0.70 NA, 40x/1.25 NA, and 63x/XX 1.40 NA objective lens. We used frame accumulation to improve signal-to-noise ratio and produce high quality confocal images. Prior to quantification, we confirmed that the isotype control slides for each staining day were negative.

Microscopy Protocol

The aim of our experiment was to identify and quantify sympathetic nerve terminals, by definition, the colocalization of two antibodies (e.g., tyrosine hydroxylase

and synapsin). We examined differences between two vascular regions, two social conditions, and two disease conditions, an experiment representing several hundred slides. Differences in the nature of the vascular tissue (e.g., presence of disease) introduced variability in the staining intensity and non-specific staining/ background noise; thus, we were in need of a valid and reproducible data processing and quantification method.

After extensive research, we created a standardized procedure (Noller et al., in preparation) for acquiring, processing, and quantifying small biological structures, using currently available open-access software (i.e., FIJI/ Image J). Each step is detailed below, starting with an outline of the most important step, image acquisition.

Imaging: Optimizing Acquisition

Lateral Resolution: Arguably more important than quantification is correct acquisition of data. Microscope settings must be customized for the structure of interest. This can be achieved by following the principles outlined by the Rayleigh Criterion and Nyquist rate. The Rayleigh Criterion provides the minimal distance (γ), that two objects can be distinguished as separate entities, also known as the lateral XY resolution. The calculation involves a very straightforward estimation, taking into account the wavelength (λ) and numerical aperture (NA) of the lens; a commonly used equation is $\gamma = 0.61\lambda/NA$. Numerical aperture is a measure of the lens' ability to resolve fine detail in the sample, with an increase in resolution corresponding to an increase in NA.

For preliminary approximations, 500 nm can be used as a general substitute value for wavelength. Using a 10x/0.4 NA objective lens as an example, the Rayleigh Criterion

tells us that we can use this lens to resolve two objects with a distance as small as 0.763 μm (i.e., [(0.61)(500)]/.40 = 762.5 nm or 0.763 μm).

Sampling Rate: Once the required distance between objects has been identified, the next step is to determine the desired pixel size needed for sufficient sampling, provided by calculating the Nyquist rate. The general concept at this step is that one must sample between 2-3.5 times more than the theoretical smallest value. Using our previous example (i.e., 0.763/3.5), our optimal sampling rate would be achieved by using a pixel size of 0.381 μm/pixel.

However, we were interested in identifying nerve terminals with reported intervaricosity distances ranging from 2.33 – 8.21 μm (Cottee, Lavidis, & Bennet, 1996; Lavidis & Bennett, 1992). Thus, the theoretical XY resolution was much smaller than what was needed for our study. We used a conservative but practical estimate by choosing the middle value of the smallest estimates (e.g., 2.85 μm) and calculated the Nyquist sampling rate by using our smallest object of interest (i.e., 2.85/3.5 = 0.814 μm/pixel). This value gave us an optimal pixel size specific for our study, easily achieved by adjusting the settings on the microscope.

Because we were acquiring tiled images of whole blood vessels, we wanted as large a field of view as possible. Therefore, for quantification purposes, we used a fluorescent microscope with a 10x objective lens, delivering a resolution of 0.643 μm/ pixel, sufficient for our structure of interest. This automated microscope had the capability of imaging the whole slide, decreasing both acquisition time and eliminating the risk of photobleaching faced when stitching tiled images obtained using a single-view confocal microscope.

Quantification of Sympathetic Nerve Terminal Densities

We used the *Bio-Formats* plugin of FIJI/Image J to import Olympus files and saved each channel as individual .tiff files. Metamorph software was used to designate intimal and medial regions of interest (ROI). These were created using the DAPI channel/file, allowing us to create regions based on anatomical differences (e.g., the non-diseased intima is 1-2 cell layers thick with diseased regions extending beyond this area into the lumen; medial regions are delineated by the presence of an inter-elastic lamina). *Figure 1* demonstrates intimal and medial regions on representative NZW and WHHL images.

Within the WHHL group, we drew two additional regions of interest based on presence or absence of disease. H&E slides were used to independently rate lesion severity using a scale of 1-5 by a pathologist (J.Z.) blind to social condition, according to AHA classification (Stary et al., 1994; Stary et al., 1995). Using these lesion severity scores, intimal and medial regions were identified for areas of extensive disease and minimal disease in the same sections of the arch and thorax. Only one slide per animal, per aortic location was examined using this approach, as it will be shown that high reproducibility between slides was present in our experiment. In subsequent analyses, these regions will be referred to as “most” versus “least” disease, distinct from whole vessel analyses. FIJI/Image J was then used to import saved regions using the *Metamorph ROI* plugin, and for all pre-processing and analyses.

Prior to quantification, the tyrosine hydroxylase and synapsin images were processed separately to subtract background signal. Positive signals were binarized and segmented to separate touching objects. The two processed channels were combined to

produce an image containing the colocalization of both tyrosine hydroxylase and synapsin staining. Sympathetic varicosities were identified by quantifying the number of objects staining positive for both fluorescent probes. Regions stained only for tyrosine hydroxylase or only synapsin were not considered to be sympathetic nerve terminals.

Double labeled varicosities and area within designated regions of interest were quantified and recorded for each slide using the Analyze Particles and Measure features of the Image J program. For defining varicosities, a size range of 0.83 – 12.60 squared microns was used for quantification, determined as follows. An object the size of one pixel (e.g., 0.643 μm) was considered to be indistinguishable from background noise, thus, we used the area of two pixels squared as the minimum size range (e.g., 0.83 μm^2). The maximum size was determined by using the largest cross sectional length described in previous reports to estimate the circular area of the varicosity (e.g., 12.60 μm^2) (reviewed in both Gabella, 1992 and Luff, 1996).

Data Processing: Dealing with background

There are three commonly used filters used to remove background noise from images; sources of which can include optical aberrations, auto fluorescence, and/or non-specific staining. Because of the similarity among filters, we briefly describe the first two and then explain why our final choice was more appropriate for our data. The chosen filter was applied to individual channels of each image.

Smoothing Filters:

Mean Filter: Applying this filter essentially replaces a pixel value with the mean of its neighboring pixels, the "neighborhood" of which is referred to as a "kernel." A kernel can be thought of as the box around the pixel of interest, therefore, the larger the

kernel, the larger number of pixels included in the mean replacement value. A 3x3 kernel is often used as an "all purpose" size filter for both mean and median filters, at least to start. The mean filter can be beneficial, as it eliminates pixels that do not represent other surrounding pixels. However, it can be problematic as when, in our case, the ratio of specific staining to background staining is low.

Median Filter: The median filter works in a similar manner as the mean filter. Instead of replacing a pixel with the mean of the kernel, as the name implies, it uses the middle or median value. This is particularly helpful if the staining includes a lot of non-specific background or areas of extremely high pixel values (i.e., auto fluorescence due to bubbles in the mounting media). This filter tends to retain sharpness in the image.

Gaussian Blur: This filter is similar to the mean filter, except that the kernel used is the shape of a bell, or Gaussian distribution, hence the name. It uses the pixels falling under the center of the curve to create a "weighted average." This function provides a smoother image, while still maintaining sharp edges, unlike a similarly sized mean filter. It is necessary to specify the size of the filter, referred to as "sigma", which is essentially the standard deviation of the distribution.

Often the user simply applies a Gaussian filter with sigma ranging from 2-3 to smooth the image. However, we had extensive, albeit low values, of non-specific background staining and/or auto fluorescence, and decided to filter out as much of this background as possible. Using sigma = 15, we used this filter to produce a blurred image representing low intensity pixels. We then subtracted the filtered image from the original image, resulting in an image that contained only the specific staining. *Figure 2A-C* demonstrates the effects of the above mentioned process on a representative raw image.

Signal intensity problems/less-than-optimal staining

Make Binary: Because we were interested in the presence or absence of staining, we binarized the images; a process that transformed the image to where pixels were either 0 or 1 (i.e., "no" or "yes"), demonstrated in *Figure 2D*.

Watershed: The watershed process allows the user to separate touching objects and works with the concept that an image contains peaks and valleys; peaks corresponding with higher grayscale values towards the center of distinct separate objects. Thus, a valley would correspond to the space between adjacent objects, however small that might be. The watershed process theoretically fills the valleys until segmentation between objects is apparent. A common criticism of this process is that is often over-segments, producing particles that might resemble noise. However, we used a specifically defined size range during quantification allowing us to avoid counting very small particles. The effects of the watershed function are demonstrated in *Figure 3*.

Colocalization

Because we were interested in the presence of two staining markers, we used a simple method to combine the two channels of interest, both of which were individually processed as previously described. We selected both channels of interest and used the "AND" feature of Image Calculator to combine the images. The resultant image contained the overlap of the two channels, defined as colocalization. This process is demonstrated in *Figure 4A-C*.

Quantification

We imported ROIs for each slide into FIJI/Image J using the *Metamorph ROI* plugin. Using the final processed AND image, we quantified specific regions of interest

and saved individual results. The Measure option provided area measurements for the image which were used to standardize particle counts in different sized areas. Thus, we analyzed particles and measured areas for each region, resulting in a raw count and size (mm^2) for each ROI. *Figure 4D* shows an example of quantified objects.

Outcome Variables

Sympathetic innervation was defined as the total number of varicosities per total area (mm^2) of the section. Total counts and total area were defined as the sum of intimal and medial values. This ratio will simply be referred to as innervation or innervation density throughout this report.

Analytical Plan

Analyses of variance were conducted using a 2 (Rabbit Strain) x 2 (Social Environment) x 2 (Aortic Location) design. We followed significant interactions with simple effects. Simple group comparisons between rabbit strain (e.g., for behavior and disease measurements) were conducted using independent samples t-tests. Preliminary data screening using boxplots within rabbit strains indicated no extreme outliers

Finally, collapsed across social environment, within rabbit strain (e.g., NZW vs. WHHL), we used correlational analyses to examine the relationship between innervation patterns and the following parameters related to unstable social environments or disease (e.g., cortisol, cholesterol, and triglycerides).

Chapter 3: Results

Quantification of Sympathetic Innervation

Reliability

Sympathetic innervation within intimal and medial regions of the vessel was quantified using three slides within each aortic location (e.g., arch and thorax) per animal. The mean of the three slides was used for all analyses, after determining consistency across slides. Correlations between slide pairs were very high, supporting reliability in the creation of specific regions of interest, as well as our standardized data processing and measurement protocol.

Pearson's correlation coefficient (r) values between slides for intimal, medial, and total area measurements in the arch ranged from .876 to .990, while values in the thorax ranged from .937 to .991; indicating consistency among the size of specific regions of interest across slides. Correlations between slides for intimal, medial, and total counts of the arch ranged from .883 to .937, with thorax counts ranging from .896 to .930; supporting our method for data processing and measurement. See *Table 1* for specific values and comparisons.

Behavior

Although animals were subjected to the same social environments, we found significant differences in behavior between the two rabbit strains, where NZW rabbits (*Mean ± SD;* 28.0% ± 2.4) spent a larger percentage of time in affiliative behavior compared to WHHL rabbits (17.0% ± 4.0), $t(44) = -2.336$, $p < .05$. However, they spent less time in inactivity (8.6% ± 1.7) compared to WHHL animals (24.9% ± 1.0),

$t(44) = 8.431$, $p < .01$. It is notable that we did not find group differences in agonistic behavior or in other non-agonistic behavior, $p > .05$ for both comparisons. *Table 2* describes average time spent in particular behavior types by rabbit strain.

Gross Examination of Disease

Disease was quantified as the total combined area of disease in the arch and thoracic regions in mm^2. There were significant disease differences between groups, where as expected, WHHL displayed a greater combined area of disease (361.4 mm^2 ± 321) with the NZW displaying minimal early raised lesions (1.1 mm^2 ± 3), $t(21.003) = 5.266$, $p < .01$.

Within the WHHL strain, animals in the the unstable group (481.4 mm^2 ± 305) displayed a larger area of disease compared to those in the stable group (217.4 mm^2 ± 290), $t(20) = 2.065$, $p = .05$. With such a small area of disease expressed, we did not expect to find differences within the NZW group. The means hinted to a similar effect of social environment as the WHHL group, however the difference was not statistically significant, $p > .05$. *Table 2* shows a breakdown of disease by rabbit strain and social environment.

Innervation Throughout the Vessel

Sympathetic nerve terminals were present throughout both regions of the vessel. Identification of sympathetic innervation is demonstrated in *Figure 5*, showing precise labeling of synapsin, tyrosine hydroxylase, and colocalization of the two markers. Sympathetic innervation in diseased versus non-diseased animals is shown in *Figure 6*, along with binarized images identifying double-labeled objects. A representative isotype

control slide is shown in *Figure 7*, demonstrating the absence of specific staining of varicosities contrasted with the distinct staining shown in *Figure 5*.

Figure 8 shows innervation density of the aortic arch and thorax for NZW and WHHL rabbits. Results of the 2 x 2 x 2 ANOVA on innervation showed a significant interaction between rabbit strain and aortic location, $F(1, 41) = 5.59$ $p < .05$. Within the NZW group, the arch (1224 ± 289) showed greater innervation than the thorax (850 ± 198), $t(46) = 5.240$, $p < 0.01$. The WHHL group did not show mean differences in aortic location; innervation in the arch (1538 ± 287) was not different than the thorax (1473 ± 376), $p > 0.05$. For this reason, additional analyses were conducted separately for each location.

In the arch, WHHL rabbits (1538 ± 287) showed greater innervation density than NZW rabbits (1224 ± 289), $F(1, 43) = 13.289$, $p < .01$. We found this same pattern in the thorax, where WHHL rabbits (1473 ± 376) had more innervation than NZW rabbits (850 ± 198), $F(1,44) = 50.876$, $p < .001$. Overall, there was a main effect of aortic location, where the arch (1371 ± 326) was more densely innervated than the thorax (1131 ± 419), $F(1,41) = 13.353$, $p < .01$. These data strongly suggest that disease increases sympathetic innervation.

We evaluated whether social environment played an added role within the WHHL group. However, contrary to our hypotheses, we did not find any significant difference between social conditions in either the arch, $F(1,19) = .002$, or thorax, $F(1,20) = .263$, $p > .05$ for both comparisons, see *Figure 9*. Our hypothesis was that social environment would influence innervation. However, the mean difference in innervation density in the

arch between unstable (1540 ± 352) and stable (1535 ± 189) was not statistically significant. The thorax demonstrated a similar non-significant pattern of means.

Relationship between Counts and Area

In order to understand how disease and innervation were related within rabbit strains, we examined the association between the number of varicosities and intimal size, the area of the vessel that expands as disease progresses. Across both strains, we found a strong relationship between intimal counts and intimal area in the arch, $r(45) = .872$, $p < .001$. This relationship was also observed in the thorax, $r(46) = .871$, $p < .001$. When we looked within the NZW group, there was no relationship between intimal counts and intimal area in either aortic location, $p > .05$ for both comparisons (see *Figure 10*). These data are consistent with the finding that these animals did not show extensive disease. However, within the WHHL group, there was a strong relationship between intimal counts and intimal area in both the arch, $r(21) = .855$, $p < .001$, and thorax, $r(22) = .789$, $p < .001$, again supporting the notion that as disease increases, so does sympathetic innervation. This relationship is demonstrated in *Figure 10*.

We then examined the ratio of intimal area to vessel size as an additional, alternative representation of disease and found that percentage of intimal area was smaller in NZW animals compared to WHHL animals. This outcome was found in the arch (5.5% ± 1 compared to 17.8% ± 9, respectively), $t(20.234) = -6.566$, $p < .01$, as well as in the thorax, where NZW animals (6.8% ± 1) had smaller relative intimal areas compared to WHHL animals (21.4% ± 9), $t(21.107) = -7.473$, $p < .01$. This outcome further supports the idea that disease drives innervation. We did not find significant

differences in percentage of intimal size across social condition for either aortic location, $p > 0.05$ for both comparisons.

Innervation within Specific Regions of Disease

We compared regions of low and high disease within the same WHHL cross-sectional sample in order to determine whether there were differences in innervation between areas that differed in the extent of disease, and whether social environment was responsible for this effect. Two regions were evaluated, those with "most" versus "least" disease, in each animal. We confirmed significant differences in lesion severity, where, the "most diseased" regions (Arch: 3.90 ± 1.38; Thorax: 4.00 ± 1.61) had more severe lesions compared to the "least diseased" regions (Arch: 0.62 ± 1.02; Thorax: 0.14 ± 0.48) in the arch, $F(1,19) = 82.306$, $p < .001$, as well as in the thorax, $F(1,19) = 94.517$, $p < .001$, supporting the distinct nature of the two regions.

In the arch, we found a significant positive relationship between the number of varicosities and intimal area within most diseased regions, $r(21) = .757$, $p < .001$, and a trend suggesting a similar relationship in areas of least disease, $r(21) = .415$, $p = .062$. We observed equivalent results in the thorax, where intimal counts increased as intimal area increased in diseased regions, $r(21) = .766$, $p < .001$, as well as in least diseased regions, $r(21) = .680$, $p < .01$. Because the intimal area expands as disease progresses, these data suggest that innervation may be driven by extent of disease, as we observed stronger correlations in areas with extensive disease.

We did not find an effect of social environment on sympathetic innervation within specific regions. There were no significant group differences between social condition in innervation density throughout the most or least diseased regions of the arch or thorax,

$p > .05$ for all comparisons. Additionally, there was no social environment effect on number of varicosities within the intimal regions of most or least diseased areas of either aortic location, $p > .05$ for all comparisons.

In the thorax, independent of social environment, we found significantly more innervation density throughout the least diseased region compared to the most diseased region, $F(1, 19) = 9.953$, $p < .01$. The means in the arch suggested a similar pattern, but the difference was not statistically significant, $p = .146$.

We used a ratio of varicosity counts per vessel size to evaluate innervation density, however, it is possible that severity of disease may have influenced our results. After examining diseased regions further, we found a significant relationship between intimal areas and lesion severity in the most diseased regions of the arch, $r(21) = .488$, $p < .05$, and thorax, $r(21) = .609$, $p < .01$, confirming expansion of the intima as disease progressed. Additionally, in diseased regions of the thorax, there was a significant relationship between number of intimal varicosities and lesion severity, $r(21) = .445$, $p < .05$, and a trend suggesting a similar relationship in the arch, $r(21) = .371$, $p = .098$.

Taken together, these findings show an increase in nerve terminal counts as disease progresses, an outcome that may have been disguised by the necessity of adjusting for vessel size area. They also suggest that lesion severity may negatively influence the ratio we used, as advanced lesions often contain necrotic areas. That we observed a decrease in innervation density in areas of extensive disease further supports this idea.

Figure 11 demonstrates an advanced atherosclerotic lesion and typical observed necrotic areas. Indeed, when we normalized number of varicosities by specific area (i.e.,

intimal counts per intimal area), we found an inverse relationship between lesion severity and innervation in diseased regions of the arch, $r(21) = -.527$, $p < .05$, as well as thorax, $r(21) = -.548$, $p < .05$. Collectively, the data suggest that as disease worsens, sympathetic innervation increases; and that a decrease in innervation is found in severe lesions characterized by expanded intimal areas and areas of associated necrosis.

Mechanistic Role of Macrophages

Preliminary data strongly support the interrelatedness of the sympathetic nervous system and immune cells. *Figure 12* shows extensive tyrosine hydroxylase labeling throughout the entire vessel of a WHHL rabbit with advanced atherosclerosis. The triple-labeled inset of this figure demonstrates the spatial relationship of sympathetic innervation with macrophages. Importantly, this figure also highlights the potential role of macrophages in advancing atherosclerosis by way of NGF release.

Relationship between Innervation and Other Measures

We examined the relationship between sympathetic innervation and several measures related to disease (e.g., cholesterol and triglycerides) or an unstable social environment (e.g., cortisol). All measures were collected at study endpoint. Within either rabbit strain, there were no significant differences between sympathetic innervation density and any of the measures. Additionally, no relationship was found between number of varicosities and any of the measures.

Chapter 4: Discussion

The purpose of the current study was to examine vascular sympathetic innervation patterns in two strains of rabbits and to assess whether an increase in innervation density was driven by differences in social stress, atherosclerotic disease, or a combination of these two factors. We hypothesized and found that innervation density was more pronounced in major aortic regions that develop the most severe lesions; across all animals there was increased innervation in the arch compared to the thorax.

Within groups we expected that WHHL rabbits would show greater innervation in the arch compared to the thorax, with no differences in aortic area within NZW rabbits, due to the lack of NGF producing macrophages in vessels without disease. However, the data demonstrated the reverse pattern; NZW rabbits had greater innervation in the arch compared to the thorax, but there were no significant regional differences in the WHHL group. We did find minimal early lesions in the NZW group; thus, significant differences in these two regions may reflect subtle changes to the vessel.

Conversely, extensive disease throughout the WHHL group may have masked any regional differences within this group. Nonetheless, it is likely that differences observed in the NZW group simply reflect normal innervation patterns in a healthy vessel. Indeed, Ogeng'o et al. (2011) reported a decrease in aortic innervation in the descending aorta; where the thoracic region was less innervated than the arch.

Our second hypothesis that vascular innervation would be increased by the presence of disease was supported. WHHL rabbits indeed displayed greater innervation than NZW rabbits in both the arch and thoracic regions of the aorta. Within the WHHL group, correlational analyses showed a strong positive relationship between

number of intimal varicosities and intimal area, suggesting that innervation also increases as disease progresses. As expected, WHHL rabbits demonstrated increased disease compared to NZW animals; an outcome confirmed by pathology examination and supported by the finding that intimal regions of WHHL animals comprised a larger percentage of total vessel area when compared to NZW animals.

In order to examine how severity of disease influenced innervation, we narrowed our focus to specific lesion areas within WHHL rabbits. Within aortic cross-sections, we examined adjacent areas of low and high disease and found a relationship in both regions between number of varicosities and intimal area, again suggesting that innervation may be driven by extent of disease.

Our third hypothesis that social stress influenced vascular innervation was not supported. We expected, but did not find, that in the presence of disease, social stress would lead to an increase in sympathetic innervation. We found no evidence for the influence of social environment on sympathetic innervation across or within either rabbit strain, aortic location, or within specific lesions in the WHHL group. Additionally, we found no evidence for a relationship between sympathetic innervation and measures related to disease (e.g., cholesterol and triglycerides) or an unstable social environment (e.g., cortisol). This outcome implies that the differences between diseased versus non-diseased rabbits (e.g., NZW versus WHHL) was not due to hyperlipidemia. Additionally, it supports the idea that sympathetic innervation is not influenced by social stress, at least within the vasculature.

It is unknown why we found group differences in behavior, except that the WHHL rabbits appeared to be less sociable than the NZW animals. Differences between

observer scoring may account for differences in behavior, as one observer scored all activities in the WHHL group (J.G.) and a different observer scored for all NZW animals (C.N.). As previous work has demonstrated comparable stress responses between rabbit strains (Szeto et al., 2004), we believe group differences are attributable to inter-rater differences. Moreover, we did not find significant differences between strains in agonistic behavior. An increase in agonistic behavior has been linked to an increase in HPA activity (Noller et al., 2013), and thus, we expected a consequent increase in HPA activity in both strains housed in unstable social environments.

The current study demonstrates that innervation of blood vessels is more extensive than previously described. In prior reporting, catecholaminergic nerves in the aorta and carotid arteries have been predominately confined to the adventitial-medial border (Santer, 1982; Scott et al., 1992), with some nerves also reported in the transitional zone between the intimal and medial areas (Cavallotti, Bruzzone, & Mancone, 2002). Recent reports have described innervation within the media (Ogeng'o et al., 2011). However, to our knowledge, this is the first study showing dense sympathetic innervation throughout intimal and medial areas of diseased as well as non-diseased aortic blood vessels.

Differences in reported innervation patterns may also reflect different methods for identifying catecholamines. Two well-known methods include the use of formaldehyde (Falck, Hillarp, Thieme, & Torp, 1962) or glyoxylic acid (De La Torre, 1980) to histochemically induce fluorescence in monoamine containing neurons and varicosities. Although these methods are still in use and considered sensitive, modern

immunohistochemistry has provided greater specificity by allowing identification of tyrosine hydroxylase, the rate-limiting enzyme in catecholamine production.

The method of specific sympathetic labeling we employed was strengthened through the addition of staining for axon terminal proteins, such as synapsin (a protein associated with synaptic vesicles); thus making it possible to identify sympathetic varicosities. Finally, the use of size filters in quantification further strengthened our study by excluding cells that have the potential to synthesize catecholamines, such as macrophages, adipocytes, and endothelial cells (Nguyen et al., 2011; Vargovic et al., 2011; Sorriento et al., 2012, respectively). Future work could compare and contrast specificity among methods, providing standardization between investigators and bolstering the use of more current methods, such as immunohistochemistry.

Previous work strongly suggests that hyperactivity of the sympathetic nervous system can have detrimental health effects. Research has related increased sympathetic innervation to an increase in SIV disease severity (Sloan et al., 2007), and shown a direct involvement of the sympathetic nervous system with cancer metastasis (Sloan et al., 2010; Pimentel et al., 2012). Increased sympathetic innervation could exacerbate atherosclerosis, by way of activating β-adrenergic receptors on macrophages (reviewed in Madden, Sanders, & Felten, 1995), thus affecting subsequent release of NGF by activated macrophages (Caroleo et al., 2001), and perpetuating this circular process.

However, the presence of sympathetic innervation in normal as well as hyper-cholesterolemic vessels implies that sympathetic innervation may play a dual role in regulating inflammation. The initial role may involve mounting a strong immune response, but left unchecked, this process may exacerbate disease. Nevertheless,

considering the regulatory feedback displayed throughout the body, it is difficult to understand the purpose of such a destructive, self-propelling force, without considering the possibility of an alternative, compensatory role of NGF in response to injury.

It has been suggested that NGF has additional roles, other than nerve maintenance and growth (Levi-Montalcini, Skaper, Dal Toso, Petrelli, & Leon, 1996). There appears to be a relationship between NGF levels and extent of inflammation (Prencipe et al., 2014). Up-regulation of the primary NGF receptor, trkA, has been demonstrated in inflammatory states; where stimulation with LPS, a traditional macrophage activator, produced a four-fold enhancement of trkA expression in monocyte/macrophage cultures, compared to unstimulated controls (Caroleo et al., 2001). These studies imply that an increase in NGF may be a response to inflammation, and thus, solicit understanding of a possible anti-inflammatory role.

Our study suggests that enhanced sympathetic innervation, at least within the vasculature, may be a natural response to hypercholesterolemia, serving to activate macrophages. In light of very recent evidence (Prencipe et al., 2014), the SNS may also indirectly play a role in the immune system's regulatory response to hyperinflammation, by the same inflammatory cell activation; thus protecting the organism from the damaging effects of a hyperactive immune response. We describe this synergistic pathway as follows: norepinephrine released from nerve terminals serves to activate monocytes/macrophages, thereby releasing more NGF. Secreted NGF may play a dual role; perhaps by increasing innervation and maintaining nerve function, while also acting to regulate inflammation through trkA receptors on monocytes (Prencipe et al., 2014). Thus, in the case of hypercholesterolemia, the immediate response is one of clearing

oxidized lipids, while secondarily promoting an anti-inflammatory reparative response in the blood vessel.

Recent work has elucidated several important components of our proposed pathway. Prencipe et al. (2014) reported that NGF promoted the release of anti-inflammatory mediators and decreased inflammatory cytokine production in activated monocytes. Activated monocytes displayed up-regulated trkA receptors, and NGF binding to these receptors affected downstream signaling by promoting pathways inhibiting inflammation. Taken together, this recent work strongly implicates an important regulatory role of NGF in monocytes. It also implicates an indirect role of the sympathetic nervous system in regulating an intense inflammatory process. Whether chronic stress can affect NGF synthesis and/or receptor sensitivity is unknown.

Early work has long suggested a homeostatic role for NGF and has identified NGF plasticity. Research has shown that emotional stress can influence NGF (Aloe et al., 1994). Soldiers parachute jumping for the first time demonstrated an increase in peripheral NGF levels and an up-regulation of NGF receptors on peripheral mononuclear cells. It was reported that circulating NGF was higher the evening before the jump, suggesting that psychosocial factors, such as anxiety, may have contributed to this effect.

It is possible that chronic stress interrupts a natural regulatory loop, perhaps by way of influencing trkA and/or β-adrenergic receptors on macrophages. This potential stress modulatory role has been demonstrated by work from Qin and colleagues (2002). In an animal model of congestive heart failure (CHF), it was shown that elevated NE reduced both NGF and trkA levels. Specifically, they showed a relationship between NE, NGF, and the primary NGF receptor, where elevated NE led to a decrease in NGF and

trkA levels and cardiac noradrenergic innervation (Quin, Vulapalli, Stevens, & Liang, 2002). Thus, it is likely that a dynamic regulatory feedback exists to a point, and that disease states represent an interruption of this delicate balance.

That the sympathetic nervous system can influence the course of atherosclerosis is unquestioned and has been previously documented in several experimental models (Kaplan et al., 1982; McCabe et al., 2002). The mechanism responsible for this phenomenon is still unknown. Chronic sympathetic activation may influence disease indirectly by promoting an inflammatory state in the local environment. In a model of sepsis, it has been shown that epinephrine can prime macrophages to be pro-inflammatory, and that this priming was more efficient after co-stimulation with bacterial endotoxins (reviewed in Milksa, Wu, Zhou, & Wang, 2005). If this relationship exists in the vasculature, it may be that the combination of norepinephrine and hyperlipidemia produces an elevated pro-inflammatory response in atherosclerosis, with subsequent down-regulation of the normal inflammatory modulation network.

Work by Marchetti et al. (2011) has demonstrated pro and anti-inflammatory roles for different subsets of macrophages, where macrophages showing anti-inflammatory properties (M2 type) are important for tissue repair and reducing inflammation. It has also been shown that macrophage polarization is both flexible and reversible (Xu, Zhao, Daha, & van Kooten, 2013). Further research is needed to clarify factors influencing this plasticity, including the potential role of the sympathetic nervous system in regulating pro- and anti-inflammatory immune properties.

Research on macrophage biology has rapidly evolved in recent years and additional work is needed to disentangle the role of chronic stress on this conceivable

pro- and anti-inflammatory feedback loop. However, instead of attempting to target specific pathways, it may be more relevant to conceptualize autonomic innervation as a necessary regulator of homeostasis in the vasculature, where interrupting balance leads to the progression of disease. That is, individual components play synergistic roles.

It may be that fine-tuning of the sympathetic nervous system is necessary for an appropriate immune response, and that this system is equipped with self-modulating "brakes". These brakes may be in the form of receptors responding to microenvironment cues. This concept has recently been described in the sympathetic nervous system, where auto modulation was controlled by the response of a specific subtype of adrenergic receptor.

Clarke, Bhattacherjee, Tague, Hasan, & Smith, (2010) demonstrated the existence of auto-receptors on sympathetic axon terminals. Administration of β-blockers caused a subsequent increase in cardiac sympathetic innervation, with the β1 receptor shown to be responsible for this effect. It was also shown that this precise modulation was due to a very localized response; where locally synthesized norepinephrine inhibited axon growth. The results of this study demonstrate a self-regulating feedback loop influenced by, and responding to cues from the microenvironment. It was shown that blockade of β2 or α receptors did not influence innervation, implicating particular responsivity of the β1 receptor to excessive sympathetic activity.

This same receptor also plays a critical role in social stress mediated endothelial dysfunction, where Skantze et al. (1998) reported inhibition of psychosocial stress-induced endothelial damage by the application of a β1 blocker. Thus, chronic stress may exert an effect on this regulatory feedback loop by desensitizing β1 receptors or through

changing the expression of other receptors expressed within the vasculature. The role of the β adrenergic receptor in immunity has been reviewed extensively (Sanders & Straub, 2002), along with the effects of catecholamines on immunity (Madden et al., 1995), further expounding on the idea of stress-mediated immunity.

The concept that sympathetic innervation may be influenced by the microenvironment has been further supported by work showing a relationship between the sympathetic and parasympathetic nervous systems; where specifically, sympathetic innervation regulates parasympathetic release of NGF. Research has shown that NGF can be released from parasympathetic neurons in apparent response to sympathetic nerve activity; where a significant decrease in NGF was observed after sympathectomy (Hasan & Smith, 2000). Very recently, work from this group suggests a feedback loop between the sympathetic and parasympathetic branches, with a reported 82% increase in NGF levels detected after application of the non-selective β-agonist isoproterenol in a model of heart failure (Hasan & Smith, 2014). Importantly, differing effects of NE were shown in two different isoforms of NGF, where only the mature form was decreased after heart failure.

The outcome of these studies support the idea of a counter response of the parasympathetic nervous system to increased sympathetic activity. They suggest compensatory release of NGF in response to increased sympathetic activity, even implying a reparative role for NGF in disease states. Research also describes a sympathetic nervous system with precise self-regulating capabilities, a system that could theoretically self-limit NE release after a certain point by modulation of sympathetic

nerve outgrowth (Clarke et al., 2010). These studies emphasize that the delicate balance of the autonomic nervous system may be particularly susceptible to disruption.

Finally, it is also possible that sympathetic hyper innervation can also affect the microenvironment in other ways. Early work suggests that the density of sympathetic innervation affects compensatory release of other neurotransmitters from sympathetic neurons. Adler & Black (1985) observed an increase in substance P as sympathetic nerve density increased, with tyrosine hydroxylase activity remaining constant. The pro-inflammatory role of substance P has been previously described (reviewed in O'Connor et al., 2004), again demonstrating the potential immune-modulating effects of increased sympathetic innervation by different, yet integrated routes. Taken together, the effects of increased sympathetic innervation appear to involve indirect modulation and multiple pathways. Whether chronic stress can influence any of these pathways remains to be determined.

Our study had several limitations that may have influenced our results. We hypothesized that social environment would influence innervation, but the results of our study showed no effect. There are several possible reasons for this outcome, the first of which was experimental design. Although our behavioral manipulation was supported by previous work, we encountered heterogeneity in behavior, even within the distinct social environments defined in our study. Thus the effect of social environment may not have been constant across animals, resulting in heterogeneity in innervation as well. Future analyses will examine whether behavioral differences characteristic of unstable versus stable social environments (e.g., time spent in agonistic versus affiliative behavior) are related to sympathetic innervation.

If there is a relationship between social environment and sympathetic innervation in the vasculature, it may instead be due to individual personality traits, such as temperament, as opposed to artificially induced social environments. Indeed, previous work has demonstrated that socially relevant personality traits were related to sympathetic innervation, where Low Sociable monkeys had increased innervation, as well as increased NGF expression, compared to High Sociable monkeys (Sloan et al., 2008).

Moreover, seminal work examining the influence of social environment on the progression of atherosclerosis reported specific differences when comparing dominant animals in differing social environments, and dominant versus subordinate animals within an unstable social environment (Kaplan et al., 1982). Thus, examination of intrinsic traits may provide a more precise measurement of sympathetic innervation in the context of differing social environments and future work will examine whether personality traits such as aggression or affiliation predict sympathetic innervation in the vasculature.

That we did not find innervation differences between adjacent areas with extensive versus minimal disease in WHHL rabbits suggests a uniform influence of vascular sympathetic innervation equally affecting surrounding tissues. It is possible that observed differences were solely due to inherent variation in rabbit strain (e.g., WHHL versus NZW). However, correlational analyses strongly showed that innervation was related to disease but not hyperlipidemia, triglycerides, or cortisol.

It is conceivable that outside factors driving an increase in sympathetic innervation in diseased regions (e.g., NGF released by nearby macrophages) may exert a

paracrine influence to nearby tissue. Should this be true, it would explain why we found differences in innervation density between diseased versus non-diseased animals (e.g., WHHL versus NZW), but a similar extent in the number of varicosities between adjacent areas within aortic cross-sections from animals already demonstrating advanced lesions. Future studies could verify this paracrine effect by examining differences in NGF production and/or macrophage activity between advanced versus early lesions, and/or advanced lesions and adjacent tissue.

Alternatively, methodology may have influenced our results. Within diseased regions of WHHL rabbits, we found an inverse relationship between lesion severity and the ratio of intimal counts adjusting for intimal size, where sympathetic innervation decreased as the lesion progressed in the arch and thorax. While this finding seems paradoxical, further examination suggested that the true effect might have been masked by the severity of the lesion. Advanced lesions are characterized by areas of necrosis and we found no evidence of innervation in these necrotic areas. Therefore, we may have underestimated density within advanced lesions by normalizing for vessel size.

In both the arch and thorax of diseased regions, we found significant positive relationships between lesion severity and intimal area, which would be expected, as intimal area is often a bi-proxy marker of lesion advancement. Importantly, within diseased regions of the thorax, a significant positive relationship was demonstrated between number of intimal varicosities and lesion severity, with a similar trend appearing in the arch. These findings suggest that sympathetic innervation increases as disease progresses, until the lesion advances to the point of necrosis.

These findings also suggest that normalizing our data for vessel size may have masked an effect of lesion severity due to necrotic spaces associated with advanced lesions. That we found an increase in the density of minimal versus extensive diseased areas of the thorax further supports this idea, as severe lesions with necrotic areas, typically characterize regions of extensive disease. Using a ratio of the number of varicosities per total area was a necessary estimation of density. Although this ratio controlled for the potential confound of different sized vessels, it did not account for areas of necrosis.

Thus, future work can examine social environment differences after excluding necrotic area from analyses. Additionally, it is possible that necrosis indirectly affects sympathetic innervation by way of cell-to-cell signaling; that is, cells undergoing apoptosis may release factors stimulating nearby macrophages. If sympathetic hyperinnervation is a response to inflammation (e.g., wound healing), it is likely that areas surrounding advanced lesions would have increased innervation.

The results of this study demonstrate the presence of sympathetic innervation throughout healthy blood vessels. Our data show that sympathetic innervation is increased in the presence of atherosclerosis and suggest that innervation increases as disease increases. We did not find evidence for an effect of social environment on innervation density; however, in light of previously reported studies, it is plausible that social stress may exert influence in other ways, such as by interrupting regulatory networks crucial for maintaining homeostasis. While normo-sympathetic activity may serve to prime the immune system to a pro-inflammatory state, the body appears to have mechanisms in place to limit hyper innervation, thus, preventing extensive damage.

Chronic stress may thereby exert an effect by disrupting this self-regulating feedback loop.

Taken together, the intricacies of the body's natural inflammatory and anti-inflammatory systems may be particularly susceptible to the effects of chronic stress. Future work is needed to elucidate vulnerable regulatory components of this fine tuned network, as translating the molecular effects of social stress is crucial in designing therapeutic interventions targeting these pathways. Identifying this interconnected response network is relevant for cardiovascular as well as other chronic disease states. Now, more than ever, additional work is needed to uncover and understand factors influencing autonomic plasticity, with the aim of restoring balance necessary for homeostasis.

TABLE 1. Reliability Among Measurements

Area of Specific Region of Interest		Slide 1	Slide 2	Slide 3
Arch				
Intima	Slide 1	1	.983	.978
	Slide 2			.990
Media	Slide 1	1	.976	.945
	Slide 2			.962
Total	Slide 1	1	.986	.880
	Slide 2			.876
Thorax				
Intima	Slide 1	1	.988	.980
	Slide 2			.991
Media	Slide 1	1	.942	.937
	Slide 2			.943
Total	Slide 1	1	.953	.947
	Slide 2			.960
Raw Counts				
Arch				
Intima	Slide 1	1	.919	.920
	Slide 2			.937
Media	Slide 1	1	.905	.883
	Slide 2			.884
Total	Slide 1	1	.908	.896
	Slide 2			.899
Thorax				
Intima	Slide 1	1	.918	.930
	Slide 2			.929
Media	Slide 1	1	.896	.902
	Slide 2			.901
Total	Slide 1	1	.915	.923
	Slide 2			.921

TABLE 2. Behavior and Disease Measurements by Group (Mean ±SEM).

Percent Time in Behavior	**WHHL**	**NZW**	**Significance**
Agonistic behavior	36.0 (±6.8)	41.7 (±3.8)	N/S
Affiliative behavior	17.0 (±4.0)	28.0 (±2.4)	$p < 0.05$
Other non-agonistic behavior	22.1 (±3.8)	21.7 (±1.6)	N/S
Inactivity	24.9 (±1.0)	8.6 (±1.7)	$p < 0.01$
Total Disease (mm^2)	**WHHL**	**NZW**	
	361.4 (±68.4)	1.1 (±0.6)	$p < 0.01$
Total Lesion Area by Social Environment (mm^2)			
	Unstable	**Stable**	
WHHL	481.4 (±88.1)	217.4 (±91.8)	$p = 0.05$
NZW	1.8 (±0.9)	0.2 (±0.2)	N/S

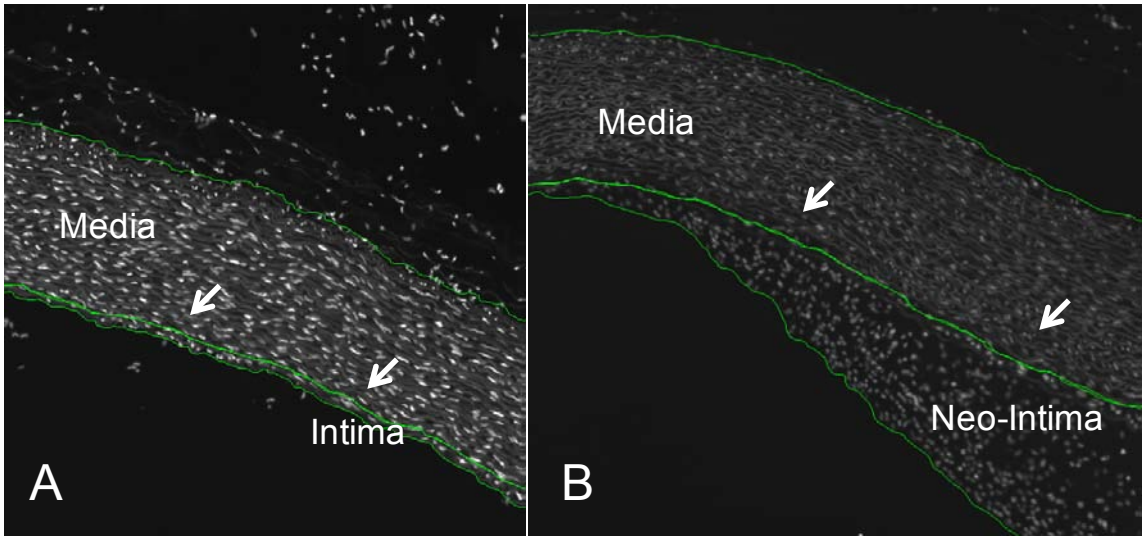

Figure 1. DAPI images for NZW (A) and WHHL (B) rabbits. Specific intimal and medial regions are outlined in green. Note the normal 1-2 cell intimal layer (A), as opposed to the expanded neo-intima in the presence of disease (B). Arrows indicate inter-elastic lamina separating intimal and medial layers.

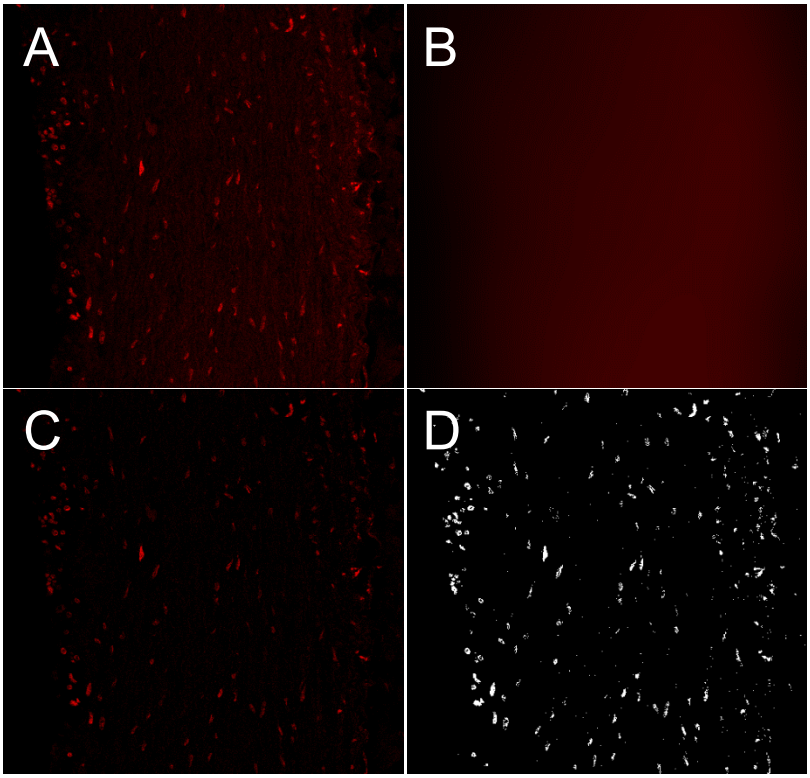

Figure 2. Figures showing image processing method on a representative tyrosine hydroxylase image. A: Raw image; B: Result of sigma 15 Gaussian filter, enhanced to show detail of background. Note very blurred image representing low intensity pixels; C: Result of background subtraction. Note the retention of specific staining and elimination of low-intensity background; D: Binary image after background subtraction. Note the retention of specific staining, while essentially transforming data into "yes" or "no" pixels.

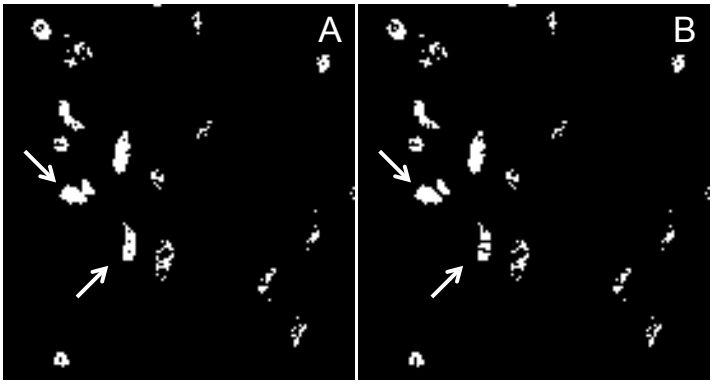

Figure 3. Close up of binary image before (L) and after applying the watershed function (R). Arrows note separation of touching objects.

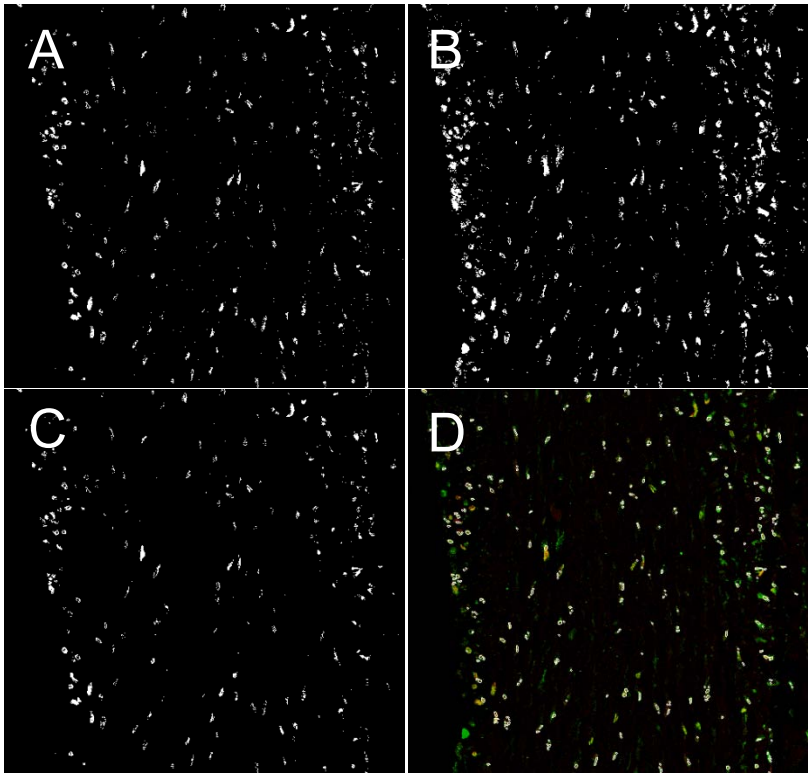

Figure 4. From left-right; binarized images of TH, synapsin, and colocalization. Overlay image showing analyzed particles in white. Note the exclusion of very small or very large particles, defined by a size filter.

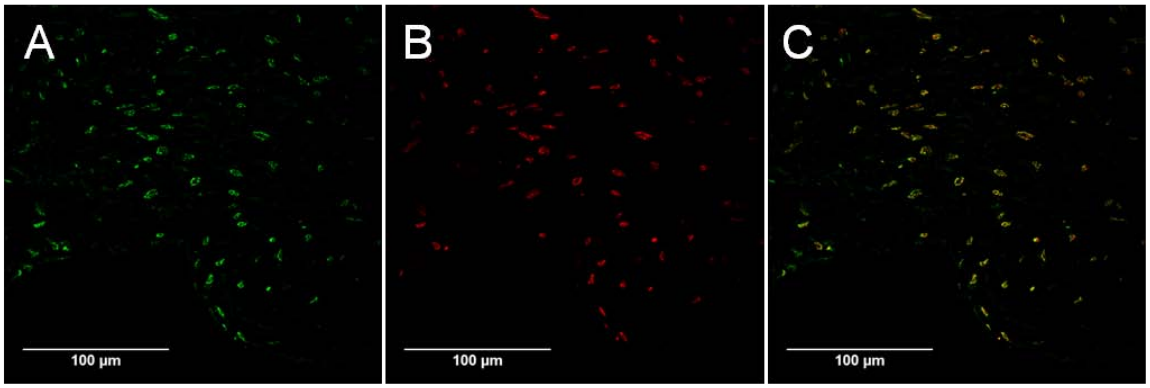

Figure 5. 40x confocal image demonstrating identification of sympathetic nerve terminals. Synapsin immunofluorescence (A) shown in green, tyrosine hydroxylase (B) shown in red, and colocalization (C) indicative of sympathetic nerve terminals.

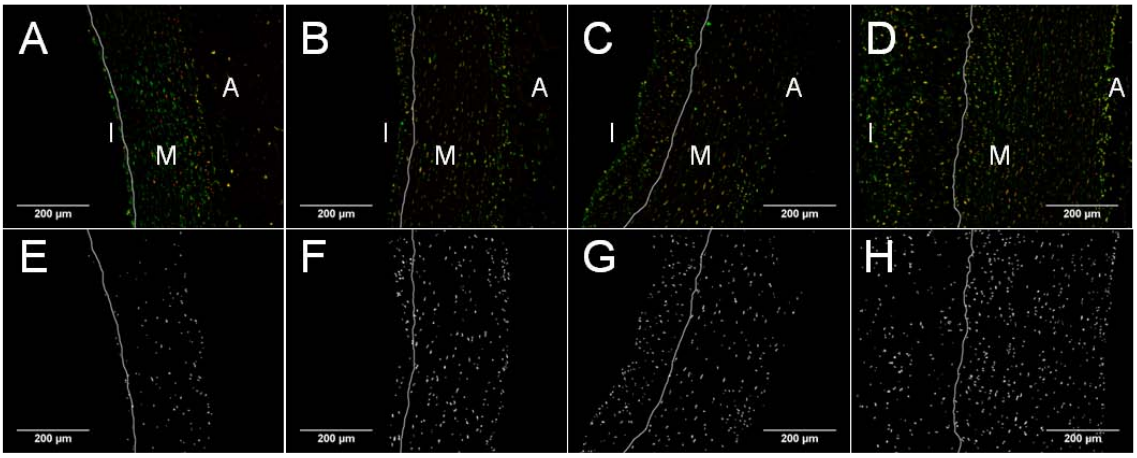

Figure 6. 20x confocal images demonstrating sympathetic innervation in diseased versus non-diseased animals. From L-R, A: NZW rabbit with no disease; B: WHHL rabbit with early disease; C: WHHL rabbit with moderate disease; D: WHHL rabbit with extensive disease. Sympathetic innervation is indicated in yellow by the colocalization of synapsin (green) and tyrosine hydroxylase (red). Panels E – H are binarized images of respective A-D panels; objects represent double-labeled nerve terminals. Intimal (I), medial (M), and adventitial (A) regions of the vessel are designated, with the inter-elastic lamina separating intimal and medial regions drawn in white. Note the increase in sympathetic innervation within the intima as disease progresses.

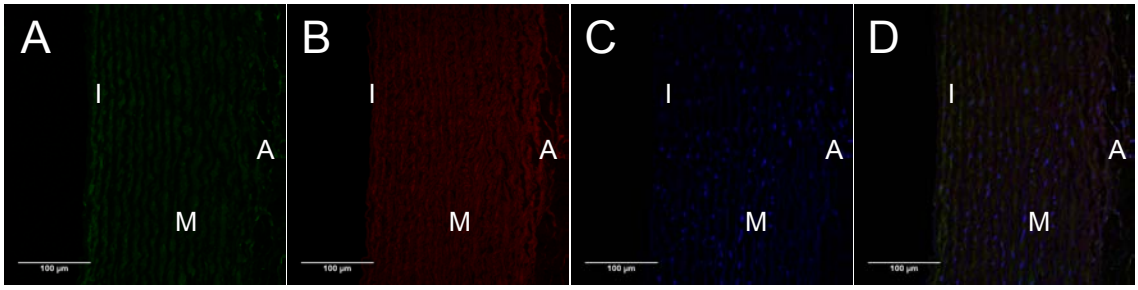

Figure 7. 40x confocal images of a typical isotype control slide. Panels A-C show individual channels; synapsin (A), tyrosine hydroxylase (B), DAPI (C), and merge (D). Intimal (I), medial (M), and adventitial (A) regions of the vessel are designated. Note the absence of specific staining. Also note that these are raw images without any background subtraction processing.

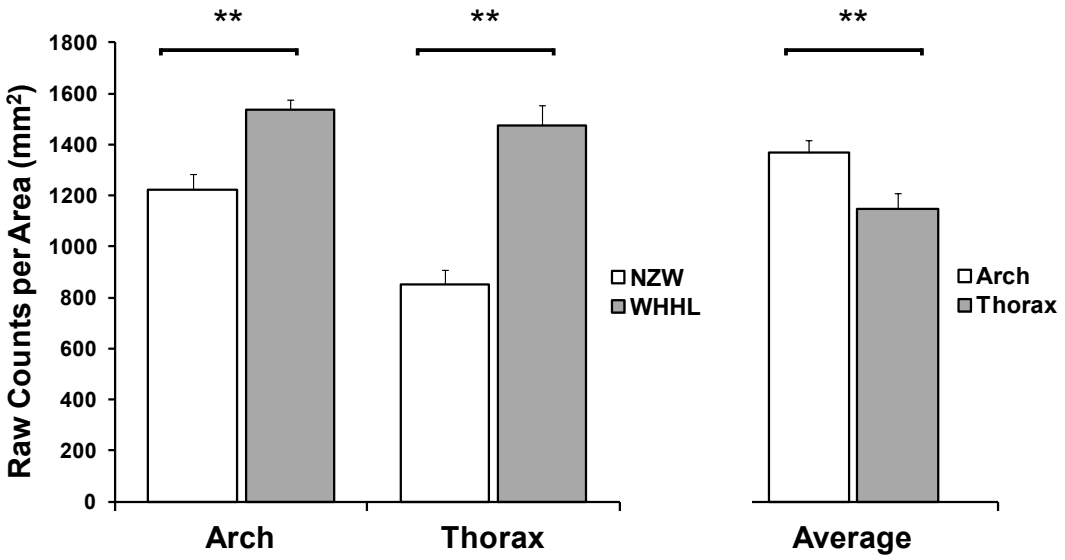

Figure 8. Sympathetic innervation density throughout the aorta. Values represent the ratio of number of varicosities per area (mm^2). Overall, WHHL displayed increased innervation compared to NZW rabbits, in both the arch and thoracic aortic areas. Additionally, across rabbit strains, the arch was more innervated than the thorax.

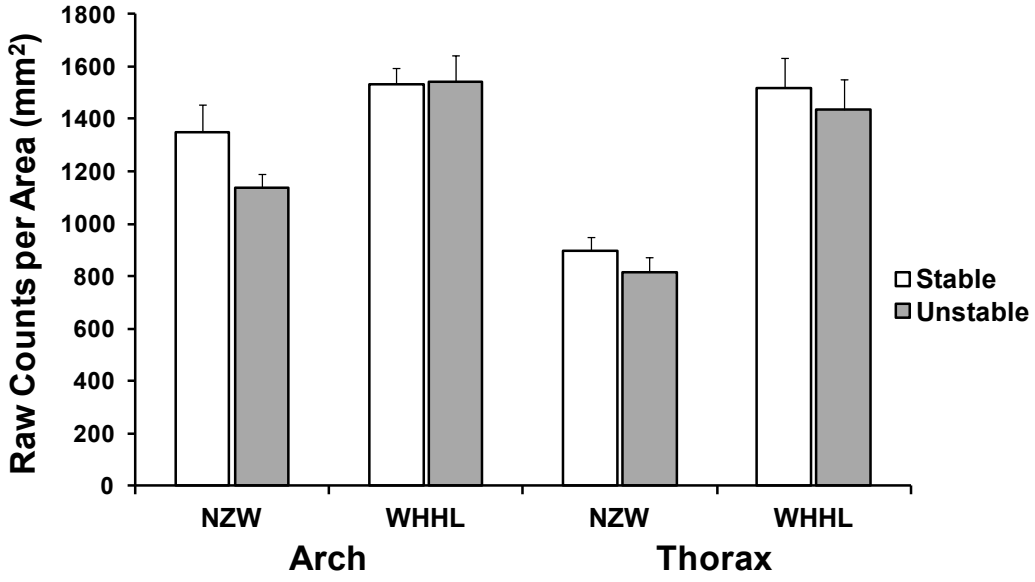

Figure 9. Sympathetic innervation density across social conditions. Values represent the ratio of number of varicosities per area (mm^2). Within either rabbit strain, there was no significant difference between social conditions for the arch or thoracic aortic areas, $p > 0.05$.

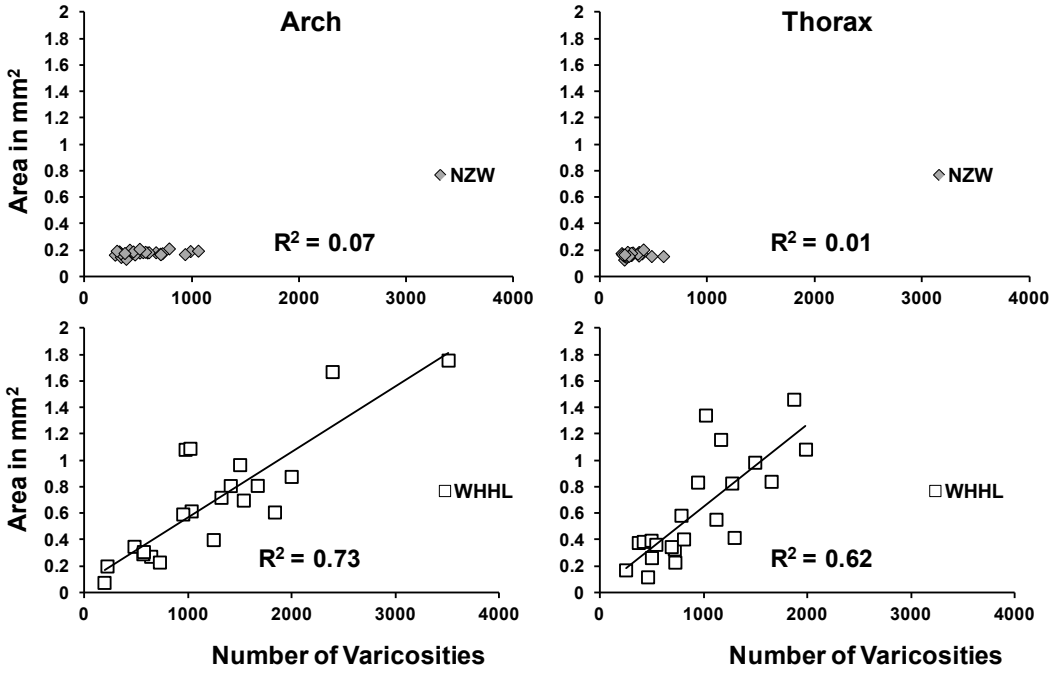

Figure 10. Graphs demonstrating the relationship between varicosities and area within the intima of the arch (L) and thorax (R). Across rabbit strain, a significant relationship showing an increase in varicosities as intimal area increased was found; this relationship existed for the arch and thorax, $p < .05$ for both comparisons, not shown. Within rabbit strains, there was no relationship in either aortic area for NZW rabbits, however, WHHL rabbits showed a strong positive relationship in both the arch and thorax, $p < .05$ for both comparisons.

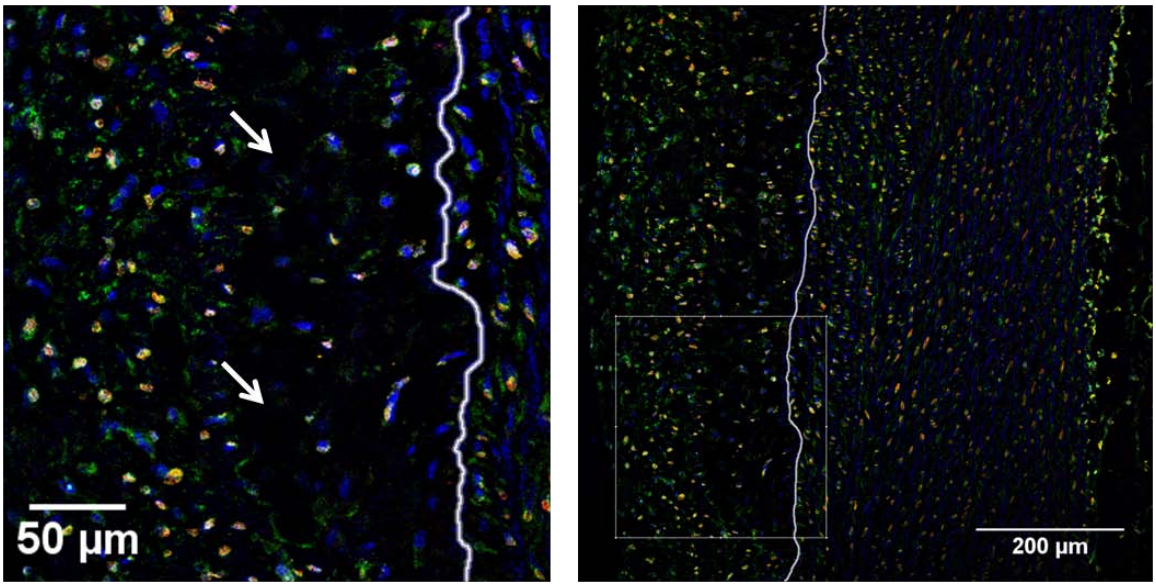

Figure 11. 20x confocal image demonstrating a WHHL rabbit with extensive atherosclerosis. Inset shows necrotic region characteristic of an advanced lesion. Sympathetic innervation is indicated in yellow by the colocalization of synapsin (green) and tyrosine hydroxylase (red). Cell nuclei are shown in blue, with the inter-elastic lamina separating intimal and medial regions drawn in white. Arrows indicate necrotic regions devoid of DAPI staining.

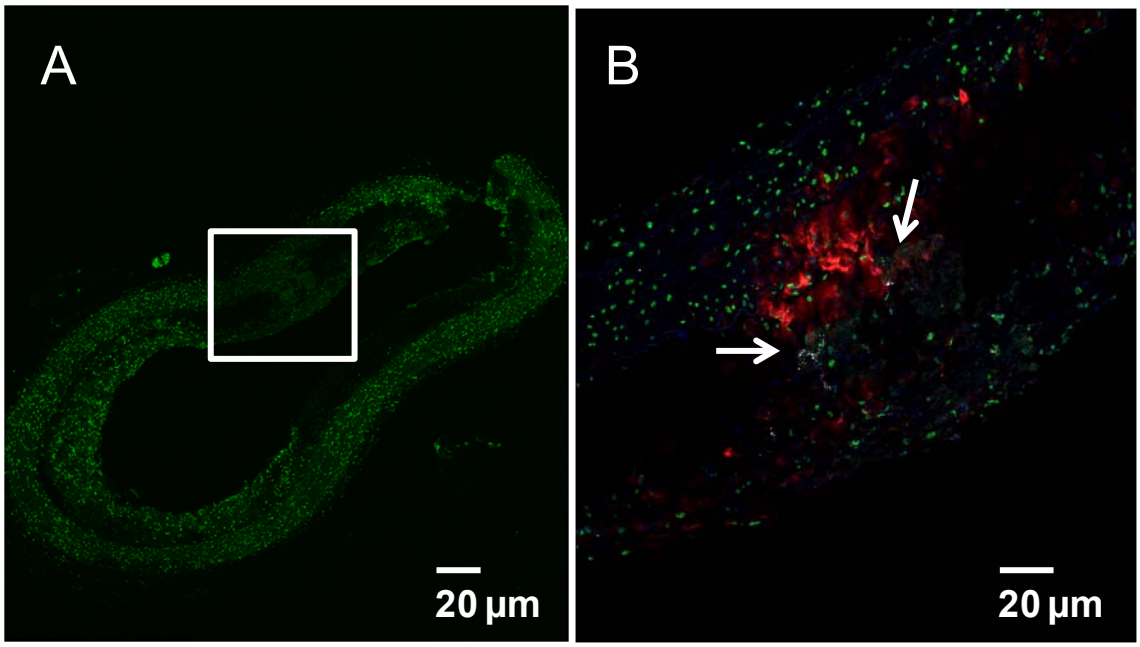

Figure 12. WHHL rabbit with extensive atherosclerosis. Panel A: 20X tiled image with tyrosine hydroxylase indicated in green. Note extensive catecholaminergic influence throughout the vessel; B: Triple labeled 40X image of region from panel A inset showing SNS varicosities (TH, green), macrophages (RAM-11, red), and NGF (white) in close proximity. Arrows point to specific NGF staining.

References

Adler, J.E., & Black, I.B. (1985). Sympathetic neuron density differentially regulates transmitter phenotypic expression in culture. *Proc. Natl. Acad. Sci. USA*, 82, 4296-4300.

Aloe, L., Bracci-Laudiero, L., Alleva, E., Lambiase, A., Micera, A., & Tirassa, P. (1994). Emotional stress induced by parachute jumping enhances blood nerve growth factor levels and the distribution of nerve growth factor receptors in lymphocytes. *Proc. Natl. Acad. Sci. USA*, 91, 10440-10444.

Aliev, G., Castellani, R.J., Petersen, R.B., Burnstock, G., Perry, G., & Smith, M.A. (2004). Pathobiology of familial hypercholesterolemic atherosclerosis, *J. Submicrosc. Cytol. Pathol*., 36, 225-240.

Barth, J., Schneider, S., & Von Känel, R. (2010). Lack of social support in the etiology and the prognosis of coronary heart disease: a systematic review and meta-analysis. *Psychosom Med*, 72, 229-238.

Bondjers, G. (1994). Anti-atherosclerotic effects of beta-blockers. *European Heart Journal*, 15, 8-15.

Buja, L.M., Kita, T., Goldstein, J.L., Watanabe, Y., & Brown, M.S. (1983). Cellular pathology of progressive atherosclerosis in the WHHL rabbit. An animal model of familial hypercholesterolemia. *Arteriosclerosis, Thrombosis, and Vascular Biology*, 3, 87-101. doi: 10.1161/01.ATV.3.1.87

Caroleo, M.C., Costa, N., Bracci-Laudiero, L., & Aloe, L. (2001). Human monocyte/macrophages activate by exposure to LPS overexpress NGF and NGF receptors. *J Neuroimmunol*, 113,193-201.

Cavallotti, C., Bruzzone, P., & Mancone, M. (2002). Catecholaminergic nerve fibers and β-adrenergic receptors in the human heart and coronary vessels. *Heart Vessels*, 17, 30-35.

Clarke, G.L., Bhattacherjee, A., Tague, S.E., Hasan, W., & Smith, P.G. (2010). β-adrenoceptor blockers increase cardiac sympathetic innervation by inhibiting autoreceptor suppression of axon growth. *The Journal of Neuroscience*, 30, 12446-12454.

Cohen, S., Kaplan, J.R., Cunnick, J.E., Manuck, S.B., & Rabin, B.S. (1992). Chronic social stress, affiliation, and cellular immune response in nonhuman primates. *Psychol Sci*, 3, 301-304.

Cottee, L.J., Lavidis, N.A., & Bennet, M.R. (1996). Spatial relationships between sympathetic varicosities and smooth muscle cells in the longitudinal layer of the mouse vas deferens. *Journal of Neurocytology*, 25, 413-422.

Danesh, J., Whincup, P., Walker, M., Lennon, L., Thomson, A., Appleby, P… & Pepys, M.B. (2000). Low grade inflammation and coronary heart disease: prospective study and updated meta-analyses, *BMJ*, 321, 199-204.

De La Torre, J.C. (1980). An improved approach to histofluorescence using the SPG method for tissue monoamines. *Journal of Neuroscience Methods*, 3, 1-5.

DeVries, A.C., Glasper, E.R., & Detillion, C.E. (2003). Social modulation of stress responses. *Physiol Behav*, 79, 399-407.

Falck, B., Hillarp, N.A., Thieme, G., & Torp, A. (1962). Fluorescence of catecholamines and related compounds condensed with formaldehyde. *Journal of Histochemistry and Cytochemistry*, 10, 348-354.

Fariñas, I. (1999). Neurotrophin actions during the development of the peripheral nervous system. *Microsc Res Tech*, 45, 233-42.

Frishman, W.H. (2003). Beta-adrenergic blockers. *Circulation*, 107, e117-e119.

Gabella, G. (1992). Fine structure of post-ganglionic nerve fibres and autonomic neuroeffector junctions. In: Burnstock, G., Hoyle C.H.V. (eds) Autonomic neuroeffector mechanisms. Harwood Academic, Chur, Switzerland, pp 1-31.

Gidron, Y. & Ronson, A. (2008). Psychosocial factors, biological mediators, and cancer prognosis: a new look at an old story. *Curr Opin Oncol*, 20, 386-392.

Go, A.S., Mozaffarian, D., Roger, V.L., Benjamin, E.J., Berry, J.D., Blaha, M.J… & Turner, M.B. (2014). Heart disease and stroke statistics – 2014 update: a report from the American Heart Association. *Circulation*, 128, 1-267.

Gulliksson, M., Burell, G., Vessby, B., Lundin, L., Toss, H., & Svärdsudd, K. (2011). Randomized controlled trial of cognitive behavioral therapy vs standard treatment to prevent recurrent cardiovascular events in patients with coronary heart disease: Secondary prevention in Uppsala Primary Health Care Project (SUPRIM). *Arch Intern Med*, 171, 134-140.

Hasan, W., & Smith, P.G. (2000). Nerve growth factor expression in parasympathetic neurons: regulation by sympathetic innervation. *European Journal of Neuroscience*, 12, 4391-4397.

Hasan, W., & Smith, P.G. (2014). Decreased adrenoceptor stimulation in heart failure rats reduces NGF expression by cardiac parasympathetic neurons. *Autonomic Neuroscience: Basic and Clinical*, 181, 13-20.

Hemingway, H., & Marmot, M. (1999). Evidence based cardiology: Psychosocial factors in the aetiology and prognosis of coronary heart disease. Systemic review of prospective cohort studies. *BMJ*, 318, 1460-1467.

Heron, M. Deaths: Leading Causes for 2009. National Vital Statistics Report; vol 61 no 7. Hyattsville, MD: National Center for Health Statistics. 2012.

Heron, M. Deaths: Leading Causes for 2010. National Vital Statistics Report; vol 62 no 6. Hyattsville, MD: National Center for Health Statistics. 2013.

Hijmering, M.L., Stroes, E.S.G., Olijhoek, J., Hutten, B.A., Blankestijn, P.J., & Rabelink, T.J. (2002). Sympathetic activation markedly reduces endothelium-dependent, flow-mediated vasodilation. *J Am Coll Cardiol*, 39, 683-688.

House, J.S., Landis, K.R., & Umberson, D. (1988). Social relationships and health. *Science*, 241, 540-545.

Hoyert, D.L., Xu, J. Deaths: Preliminary Data for 2011. National Vital Statistics Report; vol 61 no 6. Hyattsville, MD: National Center for Health Statistics. 2012.

Kaplan, R.M. (2009). Health psychology: where are we and where do we go from here? *Mens Sana Monogr*, 7(*1*), 3-9.

Kaplan, J.R., Manuck, S.B., Clarkson, T.B., Lusso, F.M., & Taub, D.M. (1982). Social status, environment, and atherosclerosis in cynomolgus monkeys. *Arteriosclerosis, Thrombosis, and Vascular Biology*, 2, 359-368.

Kaplan, J.R., Manuck, S.B., Clarkson, T.B., Lusso, F.M., Taub, D.M., & Miller, E.W. (1983). Social stress and atherosclerosis in normocholesterolemic monkeys. *Science*, 220, 733-735.

Kaplan, J.R. & Manuck, S.B. (1999). Status, stress, and atherosclerosis: the role of environment and individual behavior. *Ann N Y Acad Sci*, 896,145-161.

Koenig, W., Meisinger, C., Baumert, J., Khuseyinova, N., & Löwel, H. (2005). Systemic low-grade inflammation and risk of coronary heart disease: results from the MONICA/KORA Augsburg Cohort Studies, *Gesundheitswesen*, 67, S62-S67.

Kreulen, D.L. (2003). Properties of the venous and arterial innervation in the mesentery. *J. Smooth Muscle Res*., 39, 269-279.

Laine, P., Naukkarinen, A., Heikkilä, L., Penttilä, A., & Kovanen, P.T. (2000). Adventitial mast cells connect with sensory nerve fibers in atherosclerotic coronary arteries. *Circulation*, 101, 1665-1669.

Lavidis, N.A., & Bennet, M.R. (1992). Probabilistic secretion of quanta from visualized sympathetic nerve varicosities in mouse vas deferens. *Journal of Physiology*, 454, 9-26.

Lesserman, J., Petitto, J.M., Golden, R.N., Gaynes, B.N., Gu, H., Perkins, D.O… & Evans, D.L. (2000). Impact of stressful life events, depression, social support, coping, and cortisol on progression to AIDS. *Am J Psychiatry*, 157, 1221-1228.

Levi-Montalcini, R. (1987). The nerve growth factor 35 years later. *Science*, 237, 1154-62.

Levi-Montalcini, R., Skaper, S.D., Dal Toso, R., Petrelli, L., & Leon, A. (1996). Nerve growth factor: from neurotrophin to neurokine. *Trends Neurosci*., 19, 514-520.

Libby, P. (2012). History of discovery: inflammation in atherosclerosis. *Arterioscler Thromb Vasc Biol*, 32(9): 2045–2051.

Libby, P., Ridker, P.M., & Maseri, A. (2002). Inflammation and atherosclerosis. *Circulation*, 105, 1135-1143.

Libby, P., Ridker, P.M., & Hansson, G.K. (2009). Inflammation in atherosclerosis: from pathophysiology to practice. *J Am Coll Cardiol*, 54, 2129-2138.

Libby, P., Ridker, P.M., & Hansson, G.K. (2011). Progress and challenges in translating the biology of atherosclerosis. *Nature*, 473, 317-325.

Libby, P. & Theroux, P. (2005). Pathophysiology of coronary artery disease. *Circulation*, 111, 3481-3488.

Liu, Y.B., Wu, C.C., Lu, L.S, Su, M.J, Lin, C.W, Lin, S.F… & Lee, Y.T. (2003). Sympathetic nerve sprouting, electrical remodeling, and increased vulnerability to ventricular fibrillation in hypercholesterolemic rabbits. *Circulation Research*, 92, 1145-1152.

Lockley, R.M. (1961). Social structure and stress in the rabbit warren. *J Anim Ecol*, 30, 385-423.

Luff, S.E. (1996). Ultrastructure of sympathetic axons and their structural relationship with vascular smooth muscle. *Anatomy and Embryology*, 193, 515-531.

Luo, T.Y, Wu, C.C, Liu, Y.B, Fu, Y.K, & Su, M.J. (2004). Dietary cholesterol affects sympathetic nerve function in rabbit hearts. *Journal of Biomedical Science*, 11, 339-345.

Madden, K.S., Sanders, V.M., & Felten, D.L. (1995). Catecholamine influences and sympathetic neural modulation of immune responsiveness. *Annu. Rev. Pharmacol. Toxicol*, 35, 417-48.

Marchetti, V., Yanes, O., Aguilar, E., Wang, M., Friedlander, D., Moreno, S… & Friedlander, M. (2011). Differential macrophage polarization promotes tissue remodeling and repair in a model of ischemic retinopathy. *Scientific Reports*, 76, 1-12.

McCabe, P.M., Gonzales, J.A., Zaias, J., Szeto, A., Kumar, M., Herron, A.J., & Schneiderman, N. (2002). Social environment influences the progression of atherosclerosis in the Watanabe Heritable Hyperlipidemic Rabbit. *Circulation*, 105, 354-359.

Milksa, M., Wu, R., Zhou, M., & Wang, P. (2005). Sympathetic excitotoxicity in sepsis: pro-inflammatory priming of macrophages by norepinephrine. *Frontiers in Bioscience*, 10, 2217-2229.

Mokdad, A.H., Marks, J.S., Stroup, D.F., & Gerberding, J.L. (2004). Actual causes of death in the United States, 2000. *JAMA*, 291, 1238-1245.

Mouton, P.R. (2002). Principles and practices of unbiased stereology: an introduction for bioscientists. Johns Hopkins University Press: Baltimore.

Murphy, S.L., Xu, J., & Kochanek, K.D. Deaths: Final Data for 2010. National Vital Statistics Report; vol 61 no 4. Hyattsville, MD: National Center for Health Statistics. 2013.

Mykytowycz, R. & Hesterman, E.R., 1975. An experimental study of aggression in captive European rabbits, *Orycytolagus Cuniculus* (L.). *Behavior*, 52, 104-123.

Nguyen, K.D., Qiu, Y., Cui, X., Sharon Goh, Y.P., Mwangi, J., David, T… & Chawla, A. (2011). Alternatively activated macrophages produce catecholamines to sustain adaptive thermogeneis. *Nature*, 480, 104-109.

Noller, C.M., Boulina, M., McNamara, G., Szeto, A., McCabe, P.M., & Mendez, A.J. (2014). A Practical Guide for Imaging and Quantifying Small Biological Structures. Manuscript in preparation.

Noller, C., Szeto, A., Mendez, A.J., Llabre, M., Gonzales, J., Rossetti, M… & McCabe, P.M. (2013). The influence of social environment on endocrine, cardiovascular and tissue responses in the rabbit. *Int J Psychophysiol*, 88, 282-288.

O'Connor, T.M., O'Connell, J., O'Brien, D.I., Goode, T., Bredin, C.P., & Shanahan, F. (2004). The role of substance P in inflammatory disease, *Journal of Cellular Physiology*, 201, 167-180.

Ogeng'o, J.A., Malek, A., & Kiama, S.G. (2011). Pattern of adrenergic innervation of aorta in goat (Capra Hircus). *J. Morphol. Sci*., 28, 81-83.

Pimentel, M.A., Chai, M.G., Le, C.P., Cole, S.W., & Sloan, E.K. (2012). Sympathetic nervous system regulation of metastasis. In Metastatic Cancer: Integrated Organ System and Biological Approach, Rahul Jandial & Kent Hunter (eds). Landes Bioscience.

Prencipe, G., Minnone, G., Strippoli, R., De Pasquale, L., Petrini, S., Caiello, I… & Bracci-Laudiero, L. (2014). Nerve growth factor downregulates inflammatory response in human monocytes through TrkA. *The Journal of Immunology*, 192, 3345-3354.

Qin, F., Vulapalli, R.S., Stevens, S.Y., & Liang, C-S. (2002). Loss of cardiac sympathetic neurotransmitters in heart failure and NE infusion is associated with reduced NGF. *Am J Physiol Heart Circ Physiol*, 282, H363-H371.

Ross, R. (1999). Atherosclerosis – an inflammatory disease. *N Engl J Med*, 340, 115-126.

Sachser, N., Dürschlag, M., & Hirzel, D. (1998). Social relationships and the management of stress. *Psychoneuroendocrinology*, 23, 891-904.

Sanders, V.M., & Straub, R.H. (2002). Norepinephrine, the β-adrenergic receptor, and immunity. *Brain, Behavior, and Immunity*, 16, 290-332.

Santer, R. M. (1982). Fluorescence histochemical observations on the adrenergic innervation of the cardiovascular system in the aged rat. *Brain Research Bulletin*, 9, 667-672.

Scott, T.M., Honey, A.C., Martin, J.F, & Booth, R.F.G. (1992). Perivascular innervation is lost in experimental atherosclerosis. *Cardioscience*, 3, 145-153.

Scheiermann, C., Kunisaki, Y., Lucas, D., Chow, A., Jang-J.E., Zhang, D… & Frenette, P.S. (2012). Adrenergic nerves govern circadian leukocyte recruitment to tissues. *Immunity*, 37, 290-301.

Schneiderman, N. (2004). Psychosocial, behavioral, and biological aspects of chronic diseases. *Curr Dir Psychol Sci*, 13, 247-251.

Skantze, H.B., Kaplan, J., Pettersson, K., Manuck, S., Blomqvist, N., Kyes, R… & Bondjers, G. (1998). Psychosocial stress causes endothelial injury in cynomolgus monkeys via β1-adrenoceptor activation. *Atherosclerosis*, 136, 153-161.

Sloan, E.K., Capitanio, J.P., Tarara, R.P., Mendoza, S.P., Mason, W.A., & Cole, S.W. (2007). Social stress enhances sympathetic innervation of primate lymph nodes: mechanisms and implications for viral pathogenesis. *J Neurosci*, 27, 8857-8865.

Sloan, E.K., Capitanio, J.P., & Cole, S.W. (2008). Stress-induced remodeling of lymphoid innervation. *Brain Behav Immun*, 22, 15-21.

Sloan, E.K., Capitanio, J.P., Tarara, R.P., Cole, S.W. (2008). Social temperament and lymph node innervation. *Brain Behav Immun*, 22, 717-26.

Sloan, E.K., Priceman, S.J., Cox, B.F., Yu, S., Pimentel, M.A., Tangkanangnukul, V…. & Cole, S.W. (2010). The sympathetic nervous system induces a metastatic switch in primary breast cancer. *Cancer Research*, 70, 7042-7052.

Sorriento, D., Santulli, G., Del Giudice, C., Anastasio, A., Trimarco, B., & Iaccarino, G. (2012). Endothelial cells are able to synthesize and release catecholamines both in vitro and in vivo. *Hypertension*, 60, 129-136.

Spieker, L.E., Hürlimann, D., Ruschitzka, F., Corti, R., Enseleit, F., Shaw, S… & Noll, G. (2002). Mental stress induces prolonged endothelial dysfunction via endothelin-A receptors. *Circulation*, 105, 2817-2820.

Stary, H.C., Chandler, A.B., Glagov, S., Guyton, J.R., Insull, Jr., W., Rosenfeld, M.E.… & Wissler, R.W. (1994). A definition of initial, fatty streak, and intermediate lesions of atherosclerosis: a report from the Committee on Vascular Lesions of the Council on Arteriosclerosis, American Heart Association. *Arterioscler Thromb Vasc Biol*, 14, 840–856.

Stary, H.C., Chandler, A.B., Dinsmore, R.E., Fuster, V., Glagov, S., Insull, Jr., W… & Wissler, R.W. (1995). A definition of advanced types of atherosclerotic lesions and a histological classification of atherosclerosis: a report from the Committee on Vascular Lesions of the Council on Arteriosclerosis, American Heart Association. *Arterioscler Thromb Vasc Biol*, 15, 1512–1531.

Straub, R.H., Mayer, M., Kreutz, M., Leeb, S., Schölmerich, J., & Falkt, W. (2000). Neurotransmitters of the sympathetic nerve terminal are powerful chemoattractants for monocytes. *Journal of Leukocyte Biology*, 67, 553-558.

Szeto, A., Gonzalez, J.A., Spitzer, S.B., Levine, J.E., Zaias, J., Saab, P.G… & McCabe, P.M. (2004). Circulating levels of glucocorticoid hormones in WHHL and NZW rabbits: circadian cycle and response to repeated social encounter. *Psychoneuroendocrinology*, 29, 861-866.

Taverner, D., Mackay, I.G., Craig, K., & Watson, M.L. (1991). The effects of selective β–adrenoceptor antagonists and partial agonist activity on renal function during exercise in normal subjects and those with moderate renal impairment. *Br. J. Clin. Pharmac*., 32, 387-391

Tilan, J. & Kitlinska, J. (2010). Sympathetic neurotransmitters and tumor angiogenesis – link between stress and cancer progression. *Journal of Oncology*, vol. 2010, Article ID 539706, 6 pages.

Vargovic, P., Ukropec, J., Laukova, M., Cleary, S., Manz, B., Pacak, K., & Kvetnansky, R. (2011). Adipocytes as a new source of catecholamine production. *FEBS Letters*, 585, 2279-2284.

Wernli, G., Hasan, W., Bhattacherjee, A., van Rooijen, N., & Smith, P.G. (2009). Macrophage depletion suppresses sympathetic hyperinnervation following myocardial infarction. *Basic Res Cardiol*, 104, 681-93.

Williams, J.K., Kaplan, J.R., & Manuck, S.B. (1993). Effects of psychosocial stress on endothelium-mediated dilation of atherosclerotic arteries in cynomolgus monkeys. *J Clin Invest*, 92, 1819-1823.

Williams, J.K., Vita, J.A., Manuck, S.B., Selwyn, A.P., & Kaplan, J.R. (1991). Psychosocial factors impair vascular responses of coronary arteries. *Circulation*, 84, 2146-2153.

Xu, W., Zhao, X., Daha, M.R., & van Kooten, C. (2013). Reversible differentiation of pro- and anti-inflammatory macrophages. *Molecular Immunology*, 53, 179-186.